Supporting Information

Chemical "Pickling" of Phosphite Additives Mitigates Impedance Rise in Li-Ion Batteries.

Cameron Peebles,[1] Juan Garcia,[2] Adam P. Tornheim,[1] Ritu Sahore,[1] Javier Bareño,[1] Chen Liao, [1] Ilya A. Shkrob,[1] Hakim H. Iddir, [2] and Daniel P. Abraham[1]

[1] *Chemical Sciences and Engineering Division, Argonne National Laboratory, Argonne, Illinois, 60439, USA*

[2] *Materials Science Division, Argonne National Laboratory, Argonne, Illinois, 60439, USA*

Corresponding authors:

Ilya A. Shkrob (shkrob@anl.gov), Phone: 630-252-9516;

Hakim H. Iddir (iddir@anl.gov), Phone: 630-252-7820;

Daniel P. Abraham (abraham@anl.gov); Phone: 630-252-4332

List of Abbreviations.

ABR	Applied Battery Research
ANL	Argonne National Laboratory
ASI	area specific impedance
B3LYP	a DFT functional
CAMP	Cell analysis, Modeling and Prototyping Facility
DOE-VTP	U.S. Department of Energy's Vehicle Technologies Program
DFT	density functional theory
EC	ethylene carbonate
EMC	ethyl methyl carbonate
HPPC	hybrid pulse power characterization
HSE06	a DFT functional
Gen2	baseline electrolyte, consisting of 3:7 w/w EC and EMC with 1.2 M lithium hexafluorophosphate ($LiPF_6$)
GGA	generalized gradient approximation
LIB	lithium ion battery
NMR	nuclear magnetic resonance
NMC532	$Li_{1.03}(Ni_{0.5}Mn_{0.3}Co_{0.2})_{0.97}O_2$ cathode material
PAW	projected augmented wave
PBE	a DFT functional
PGSE	pulsed field gradient echo (NMR method for measuring diffusion coefficient)
PVdF	polyvinylidene fluoride polymer
SEI	solid electrolyte interphase
TM	transition metal
TMS	tetramethylsilane, $-SiMe_3$
TMSPi	$P(OTMS)_3$
VASP	Vienna ab initio simulation package
X	-OTMS ($-OSiMe_3$) group
Y	methoxy (-OMe) group
Z	a substituting group without coupled magnetic nuclei

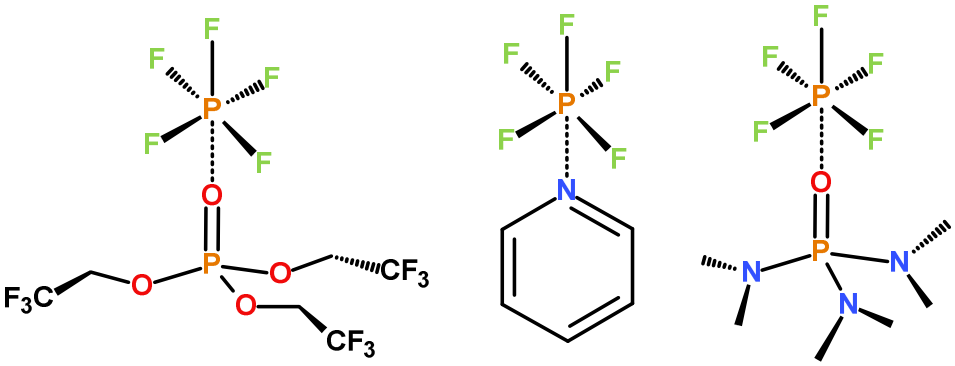

Scheme S1. Complexes of Phosphorus Pentafluoride with Donor Molecules.

Table S1.

^{19}F and ^{31}P resonances for products observed in aged 10 wt% PX_3 solutions in Gen2 (before the transformation; external reference is CD_3CN).

^{19}F species	Figure	$\delta(^{19}F)$ ppm	multiplet type	$J_{F?}$ Hz	mol% $LiPF_6$ 8 days [a]
PF_6^-		-74.86	*d*	707.8	100.0
PF_3		-35.81	*d*	1400.0	0.1
PF_2X		-34.46	*d*	1298.7	2.9
PFX_2		-35.61	*d*	1212.0	4.8
1 *(eq)*		-56.52	*ddd*	880.8, 307.6, 55.8	4.8
A		-60.35	*ddd*	914.8, 259.1, 48.2	1.6
5		-72.95	*d*	704.7	0.1
1 *(ax)*		-80.53	*d4*	778, 56.9	2.9
$PO_2F_2^-$		-85.21	*d*	928	1.2

The mixture initially contained 7.4% PX_3, 0.7% $OPHX_2$ and 0.7% OPX_3 (all concentrations are given in mol% vs $LiPF_6$. a) Days after mixing PX_3 and Gen2.

Table S1, continued. [a]

^{31}P Species	$\delta(^{31}P)$ ppm	multiplet pattern	J_{PF} Hz	mol% $LiPF_6$ Days of aging 4	6	8
PF_6^-	-145.14	*6*	707.8	100.0	100.0	100.0
PX_3	113.85	*s*	-	8.5	5.4	0.1
PF_3	102.85	*q*	1398.3	-	-	0.2
PF_2X	112.78	*t*	1299.4	0.9	1.3	2.1
PFX_2	118.32	*d*	1213.5	1.0	1.6	4.5
	115.77	*s*	-	0.4	0.4	
	115.14	*s?*	-	0.0	0.0	0.1
	68.366	*td*	221.7, 7.2	0.0	0.2	0.5
	66.55	*s*	-	-	-	-
	18.95	*4*	308.8	1.2	1.2	1.2
	7.46	*4*	308.8	1.1	1.5	1.3
1	13.18	*d4*	1398.3, 307.6	-	-	*2.5*
	10.32	*dd*	218.2, 2.4	0.4	0.6	1.1
	6.05	*d?*	304	0.3	0.4	
	-2.87	*s*	-	0.3	0.3	0.4
	-3.48	*s*	-	-	-	0.2
	-6.14	*d?*	649.7	0.2	0.3	-
imp ($OPHX_2$)	-13.65	*d*	725.98 (H)	4.0	4.1	4.2
$PO_2F_2^-$	-19.96	*t*	928.6	0.4	0.7	2.0
imp (OPX_3)	-28.08	*s*	-	2.7	-	4.1
	-28.15	*d?*	913.1	-	-	-
	-27.91	*d?*	600.8	-	-	-
1	-148.81	*d4d*	1395.9, 879.8, 790.4	-	2.4	2.5

a) PX_3 initially contained 1.6 mol% $OPHX_2$ (-14 ppm, *d*, J_{PH} 688.9 Hz) and 1.6 mol% OPX_3 (-25.7 ppm, *s*)

Table S2. Identified products in solvolysis of PXY_2 and their spectroscopic properties (X=OTMS, Y=OMe, external reference: acetone-d_6).

attribution	System	[a]	$\delta(^{19}F)$ ppm	multiplet pattern	$J_{F?}$ Hz	$\delta(^{31}P)$ ppm	multiplet pattern	J_{PF} Hz	J_{PH} Hz
PFY_2	PFH_6	a	-64.19	*d*	1202.8	131.73	*d6*	1203	10.8
$PY_2(OH)$	PH_7	-	-		-	139.64	*7*	-	10.5
$??PF_5$	PF_5	g	-61.20	*ddd*	801.3, 52.3, 11.7, 1.9	-15.51	*dd?*	797,7.4	-
PFYOP'???	PFH_3	e	-56.59	*d*	1222.1, 6.1	119.53	*ddq*	1222.5, 35.7	9.4
PF_2Y	PF_2H_3	d	-51.98	*d*	1288.5	112.99	*tq*	1288.5	8.1
PFXY	PFH_3	f	-52.12	*d*	1199.84	119.93	*dq*	1199.6	8.8
PF_2X	PF_2	h	-34.53	*d*	1299.7	112.85	*t*	1299.2	-
PF_3	PF_3	-	-35.89	*d*	1399.6	102.85	*q*	1399.6	-
$OPFY_2$	PFH_6	k	-88.59	*d*	960.8		*d6*	960.8	11.9
$PO_2F_2^-$	PF_2	b	-85.40	*d*	930.86	-19.08	*t*	933.5	-
OPF_2Y	PF_2H_3	m	-88.74	*d*	1005.6	-20.32	*dq*	1006.1	11.9

a) line lableling as in Table S3.

Tables S3. Classification of resonance lines observed in the ^{19}F and ^{31}P NMR spectra for PXY_2 (X=OTMS, Y=OMe) aged in Gen2 (external reference: acetone-d_6).

^{19}F species		System	$\delta(^{19}F)$ ppm	multiplet type	$J_{F?}$ Hz	mol% $LiPF_6$ Days of aging: 13	17	22
PF_2X	h	PF_2	-34.53	*d*	1299.7	0.70	0.21	0.02
PF_3		PF_3	-35.89	*d*	1399.6	0.19	0.39	0.35
PF_2OH?			-35.93	*d*	1401.3	-	-	0.07
PF_2OP'?			-39.15	*dd*	1314.5, 12.54	-	-	
PF_2Y	d	PF_2	-51.98	*d*	1288.5	4.85	2.69	4.23
			-51.31	*d*	1289.8	-	-	0.11
PFYX	f	PF	-52.123	*d*	1199.84	2.44	-	-
			-55.88	*dd*	1223.9, 106.4	-	-	-
			-56.08	*d*	1227.6	-	-	0.10
	e	PF	-56.59	*d*	1222.1, 6.1	7.20	0.63	-
			-57.39	*dd*	1268.2, 6.9	-	-	0.20
	g	PF	-61.20	*ddd*	801.3, 52.3, 11.7, 1.9	3.94	-	-
			-62.35	*dtdd*	743.7, 57.2, 7.7, 4	3.40	-	1.33
			-62.93	*ddd*	730.4, 50.4, 7.2	1.12	-	-
			-62.85	*ddd*	732.8, 51.8, 7.2	1.35	-	0.46
PFY_2	a	PF	-64.19	*d*	1202.8	17.3	10.69	6.78
			-65.8	*dq*	1039, 6.4	-	-	0.26
			-67.80	*dd*	1053.4, 117.1	-	-	0.51
			-72.84	*d*	707.2	-	-	0.13
			-76.82	*dt?*	806, 52.0	0.48	-	-
			-78.11	*5?*	54.4	-	-	0.25
			-81.62	*dw*	705.6	-	-	0.61
			-84.59	*dw*	912.8	1.24	-	-
PO_2F_2-	b	PF_2	-85.40	*d*	930.9	22.1	8.48	11.7
			-86.10	*dw*	904.9	-	0.20	-
			-87.22	*dw*	931.8	-	0.08	-
$OPFY_2$		PF	-88.59	*d*	960.8	0.80	0.50	5.41
OPF_2Y	m	PF_2	-88.74	*d*	1005.6	0.59	0.28	0.76

Tables S3 continued:

31P species		System	δ(^{31}P) ppm	multiplet type	J_{PF} Hz	J_{PH} Hz	mol% LiPF6 Days of aging: 13	15	17	22
PXY_2			128.23	*m*	-		1.83	1.61	0.75	-
PY_2OH		PH_7	139.65	*7*	-	10.5	2.41	1.33	0.79	-
PFY_2	**a**	PFH_6	131.73	*d6*	1203	10.8	10.2	12.3	13.31	8.60
PFXY	**f**	PFH_3	119.93	*dq*	1192.1	9.5	0.74	0.57	0.43	-
PFXOP???	**e**	PFH_3	119.88	*ddq*	1221.9,35.8	9.5	1.99	1.15	0.62	-
PF_2Y	**d**	PF_2H_3	112.99	*tq*	1288.5	8.1	1.81	2.51	3.10	4.47
PF_2X	**h**	PF_2	112.85	*t*	1299.2	-	-	-	-	-
PF_3		PF_3	102.85	*q*	1400.7	-	0.21	0.22	0.28	0.42
	y1	$PH_3(P)_2$	79.88	*ddq*	230.9, 218.8	11.9	0.46	0.43	0.44	-
	x1	$P(PH_6)_2$	36.48	*d6*	183.1	9.4	1.11	1.25	1.31	-
		PH_3H_3OH	34.31	*q4*		17.5, 11.2	9.34	10.0	11.3	11.1
	y2	$PH_3(P)_2$	28.61	*ddq?*	223.5, 4	9.5?	0.58	0.55	0.57	
			12.97	*d6*	212.1	6	0.86	0.86	0.97	1.03
		$P(O)H'H_6$	11.74	*d6*		722.3, 11.9	3.82	4.01	4.49	5.33
		$P(O)FH_6$	-4.34	*d6*	1120.6	11.9	3.43	3.98	4.55	6.07
$OPFY_2$		$P(O)FH_6$	-8.609	*d6*	960.8	11.9	0.40	0.51	0.83	6.01
		$P(O)H_3$	-18.41	*q*		11.9	0.60	0.56	0.67	0.63
OPF_2Y	**m**	$P(O)F_2H_2$	-20.32	*dq*	1006.1	11.9	-	-	-	0.95
			-18.78	*qd*		11.9, 8.3	0.46	0.34	0.26	-
PF_2O_2-	**b**	P(O)F2	-19.08	*t*	933.5		7.87	8.47	9.77	53.3
	x2	$P(PH_6)_2$	-91.1	*tq*	182.4	3.6	1.06	1.17	1.38	0.86
			129.565	*dqd?*	69.1?	10.7, 2.4	-	0.72	-	-

Table S4. ^{19}F and ^{31}P resonances for products observed in aged 10 wt% PX_3 solutions in Gen2 (after the transformation; external reference is CD_3CN).

^{19}F species	$\delta(^{19}F)$ ppm	multiplet type	$J_{F?}$ Hz	mol% $LiPF_6$ Days of aging 13	22
PF_2X	-34.47	*d*	1300.5	0.32	0.01
PF_3	-36.04	*d*	1401.5	0.14	0.04
B*	-36.13	*d*	1400.3	-	-
4*	-39.86	*dd*	1357.2,14.9	-	-
*	-40.80	*dd*	1272, 5.8	-	-
3	-42.76	*dd*	1362.5, 7.6	0.45	-
C*	-44.23	*dd*	1291.7,86	-	-
f	-57.60	*dd*	51.7, 23.8	0.75	-
h* *(eq)*	-59.71	*dd*	752.5, 54.8	-	-
a *(eq)*	-60.26	*ddd*	747, 54.8, 11.5	3.98	3.69
b *(eq)*	-60.88	*ddd*	745.1, 55.1, 9.2	1.05	1.16
c *(eq)*	-61.48	*dd4*	757.1, 57.6, 3.8	7.34	10.7
g* *(eq)*	?	*dddd*	739.4, 54.1, 8, 4.2	-	-
d *(eq)*	-62.41	*dd4*	743.1, 54.6, 3.8	0.70	3.55
e	-64.84	*dd*	1017.5, 115.1	2.48	3.43
*	-67.60	*dt*	737, 48.2	0.85	1.96
5	-72.96	*d*	707.5	0.63	0.75
a *(ax)*	-78.18	*d4*	728, 54.8	1.08	1.96
b *(ax)*	-79.14	*d4*	743.5, 54.8	2.40	4.03
c *(ax)*	-82.76	*d4*	742.0, 57.6	5.79	8.38
$PO_2F_2^-$	-85.30	*d(w)*	931.8	20.2	19.3
6*	-84.50	*d*	928.1	0.6	-
8	-86.66	*d*	969.0	7.05	8.33
10?*	-90.39	*d*	1067.3	-	-

*) Not observed in some aged samples.

Table S4, continued.

^{31}P species	δ(^{31}P) ppm	multiplet type	$J_{P?}$ Hz	mol% $LiPF_6$ Days of aging 13	22
PF_3	102.88	*q*	1399	1.73	0.20
PF_2X	112.83	*t*	1299.3	2.56	0.34
3	110.54	*td*	1362.6, 13.1	-	0.46
4*	109.92	*td*	1348.3, 10.7	-	-
10	-5.96	*ddq?*	1030, 804.7, 11.9	-	5.50
imp ($OPHX_2$)*	-13.67	*d*	723.6	1.34	-
6	-17.46	*t*	928.6	-	-
$PO_2F_2^-$	-20.11	*t*	929	6.67	20.70
9*	-27.38	*d*	732.6	-	0.18
imp (OPX_3)	-28.11	*s*	-	2.01	1.30
7	-29.24	*d*	257.5	-	-
*	-34.07	*s?*	-	-	1.85
8	-35.80	*tq?*	969.2, 8.3	2.24	7.88
PF_6^-	-145.13	*6*	709.3	100.0	100.0
5	-144.64	*4*	706.9	-	-
B	-145.28	*dqd?*	877.4, 740, 15.5	-	-
c	-146.54	*4dd*	755.8, 742.7, 8.3	1.94	7.27

*) Not observed in some aged samples.

Table S5. Classification of resonance lines observed in ^{19}F and ^{31}P NMR spectra for OPX_3 (X=OTMS) aged in Gen2 (external reference: acetone-d_6).

^{19}F species	$\delta(^{19}F)$ ppm	multiplet type	$J_{F?}$ Hz	mol% $LiPF_6$ Days of aging: 0	3	14	48
e?	-48.97	*dt*	767.9, 53.8	-	-	3.09	4.86
e?	-48.83	*ddt*	763.3, 415.4, 55.3	-	-	3.53	6.07
-	-48.08	*dt*	763.3, 55.3	-	-	1.81	2.91
-	-49.56	*dt*	769.8, 56.5	-	-	1.72	3.16
b *(eq)*	-60.03	*ddd*	745.4, 55.3, 9.2	-	0.23	3.68	4.98
d *(eq)*	-60.81	*ddd*	739.3, 53.4, 8.01	-	0.04	0.58	0.79
c *(eq)*	-60.63	*ddq*	756.8, 58, 3.8	-	-	0.19	0.98
a *(eq)*	-61.97	*ddd*	729.7, 50, 5	-	5.18	4.78	-
e	-66.75	*dtt*	739.7, 54.9, 8.01	-	0.15	2.71	4.56
5	-72.11	*d*	706.5	0.51	0.86	-	-
a *(ax)*	-74.26	*dq*	718.3, 48.1	-	4.52	-	-
d *(ax)*	-77.08	*dq*	723.6, 52.6	-	-	0.53	1.19
b *(ax)*	-78.58	*dq*	730.5, 54.9	-	0.27	3.82	5.10
c *(ax)*	-81.87	*dq*	742.3, 57.2	-	-	0.18	1.17
$PO_2F_2^-$	-84.41	*d*	930.4	0.03	0.54	4.33	7.43
8	-85.73	*d*	969.3	-	-	0.23	1.69

Table S6. Energetics of fluorination (X=OTMS, Y=OMe). [a]

$R_1R_2R_3$	P(III) phosphites $PR_1R_2R_3$		P(V) phosphates $O=PR_1R_2R_3$	
	X/F	Y/F	X/F	Y/F
X_3	0.946	-	0.718	-
FX_2	0.898	-	0.526	-
F_2X	0.585	-	0.287	-
Y_3	-	0.437	-	0.210
FY_2	-	0.343	-	0.126
F_2Y	-	0.353	-	0.020
Y_2X	0.853	0.557	0.630	0.277
FXY	0.639	0.406	0.479	0.212

a) electronic energy gain (eV) in a hypothetical gas phase reaction

$>PR + 2HF \rightarrow >PF + H_2O + RF$ (R=X, Y).

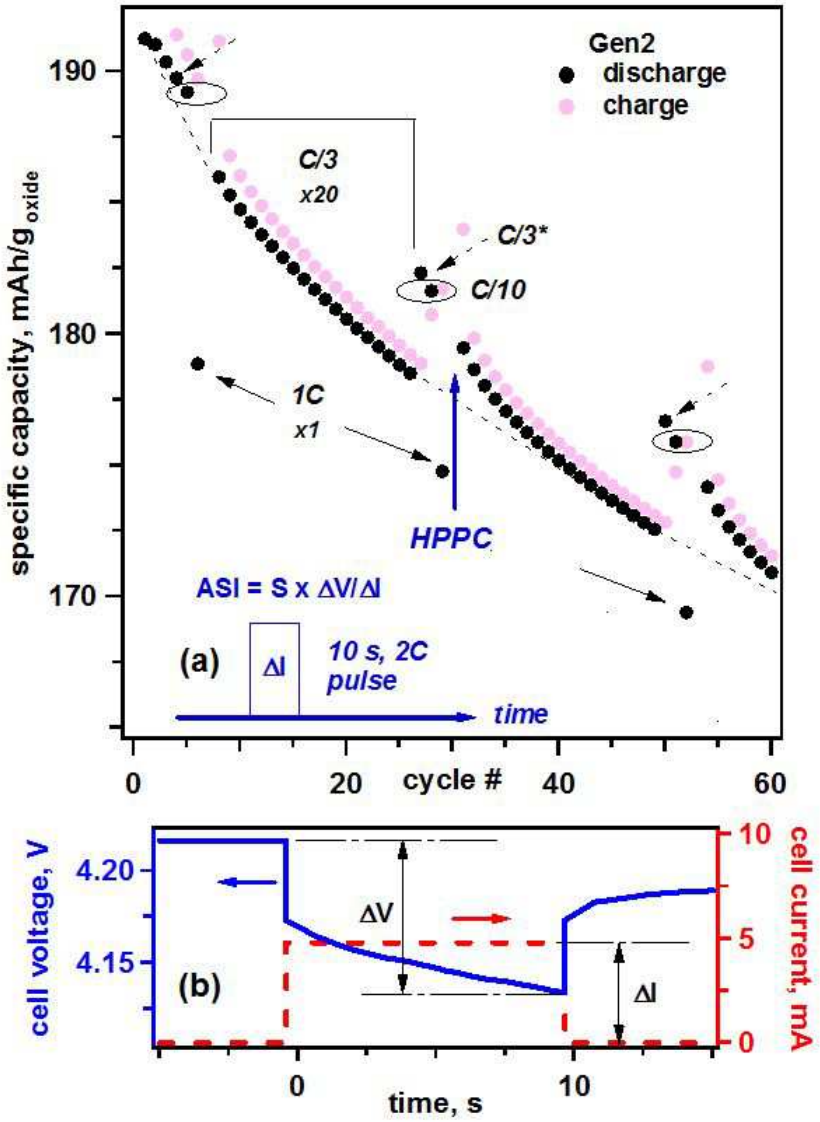

Figure S1. (a) Illustrated testing protocol (3.0-4.4 V, 30 °C). The cell charge and discharge capacity is normalized by the weight of the active material in the positive electrode. For each cell (in this case, a Gen2 cell) the testing protocol begins with four SEI formation cycles at a C/10 rate; the tests are conducted in a sequential mode, as shown in the plot. Each round consists of twenty aging cycles at a C/3 rate, which include a 3 h constant voltage hold at 4.4 V. These aging cycles are followed by a diagnostic C/3 cycle with low voltage hold on discharge (*dashed arrows*), C/10 cycle (*empty circles*) and a 1C cycle (*solid arrows*) and several hybrid pulse power characterization (HPPC) tests (shown as gaps in the plot). In the latter measurements, 10 s long, 2C current pulses (ΔI) are applied at preselected potentials as the cell discharges, and the resulting changes in the settled potential (ΔV) at the end of the current pulse are determined (see panel b for an example of such measurement). The ratio yields the cell impedance that is weighted by the electrode area (S) to yield the area specific impedance (ASI). Due to these interrupting measurements, the C/3 capacity shows the sawtooth pattern, but the tails of each segment follow on the smooth line capacity fade line.

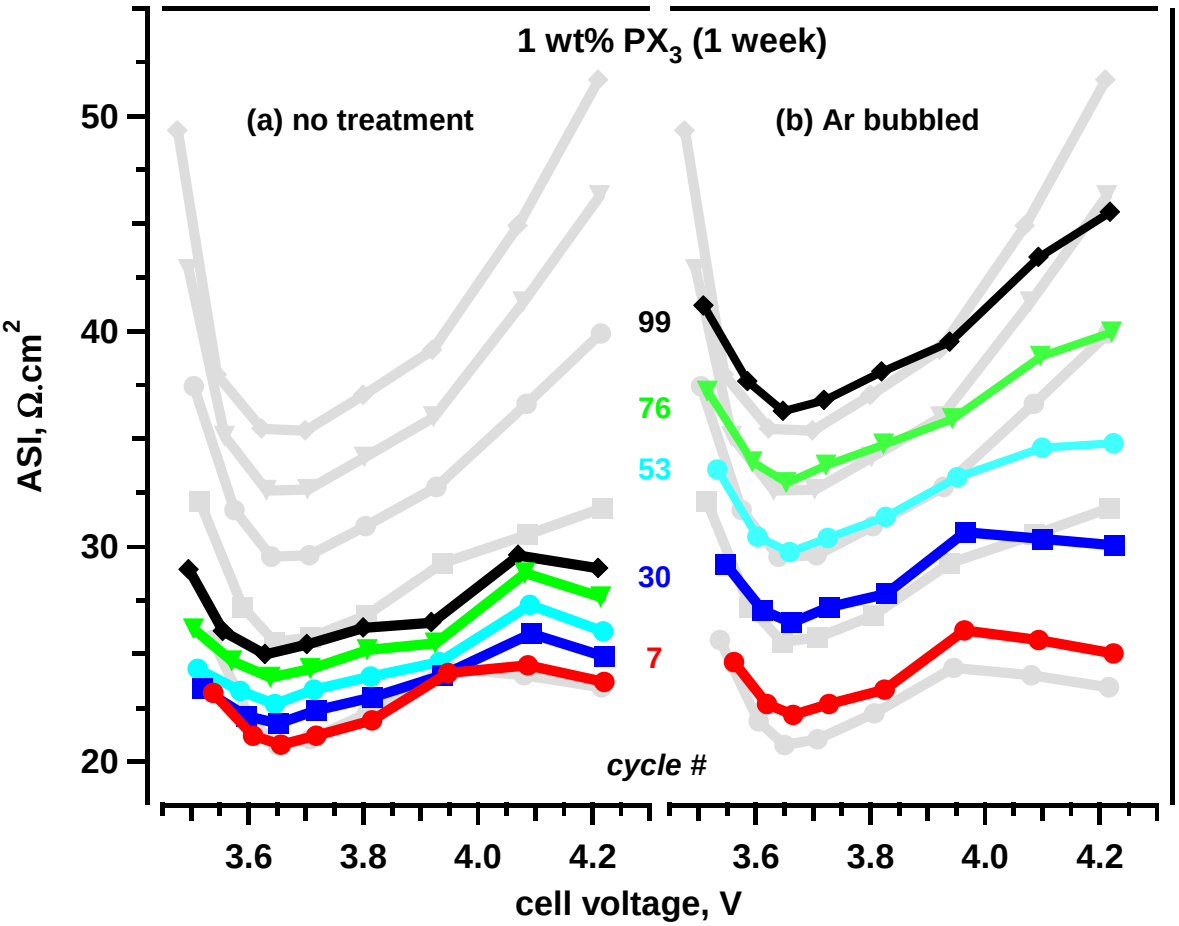

Figure S2. Like Figure 1b in the text, for 1 wt% PX_3 solution in Gen2 that was aged for one week, with (panel b) and without (panel a) Ar bubbling. Shown also in grey is the progression of ASI traces for the baseline (Gen2) electrolyte. As the volatile components of the aged electrolyte are removed, the effect on the impedance increase disappears. The number of cycles is indicated in the plot, and the same symbols are used for the traces corresponding to the same test conditions.

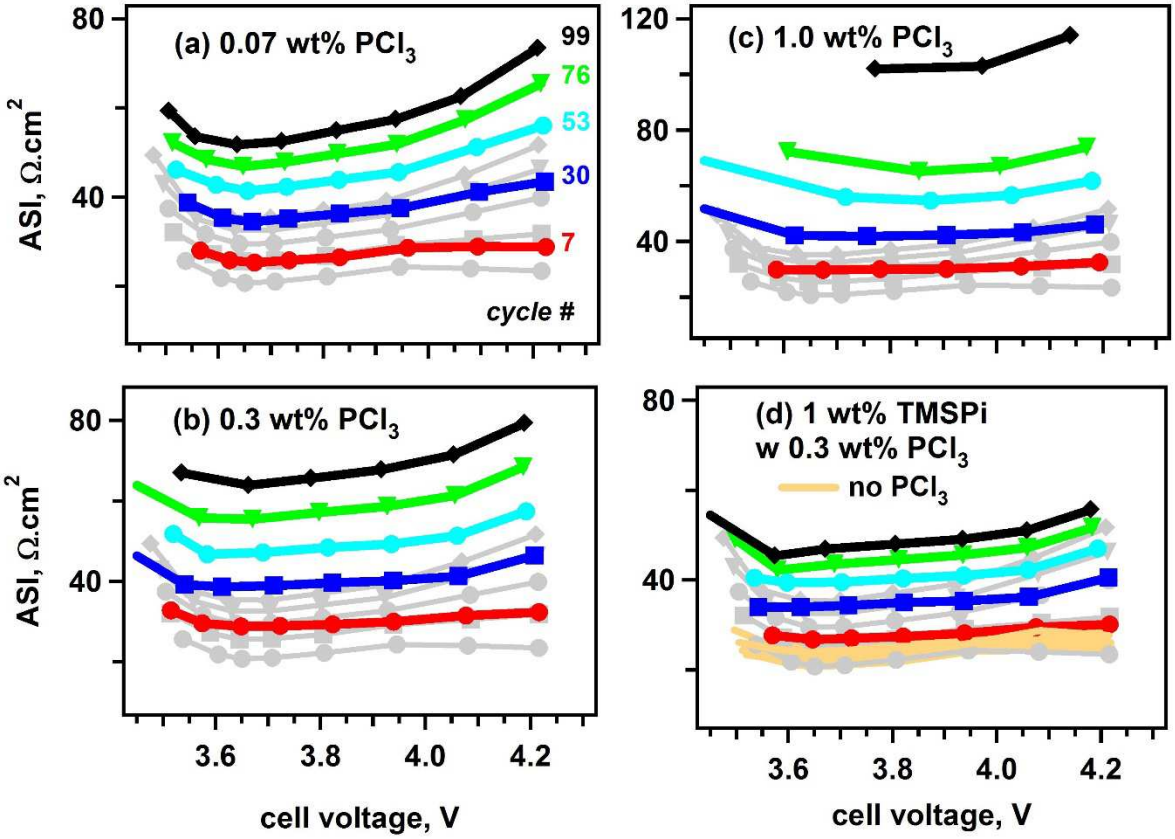

Figure S3. Like Figure 1, (a-c) for freshly prepared Gen2 solutions containing the indicated concentrations of PCl_3 and (d) freshly prepared 1 wt% PX_3 solution containing 0.3 wt% PCl_3. It is seen that with or without PX_3, PCl_3 only increases the impedance rise; at 1 wt% (panel c) this rise becomes considerable.

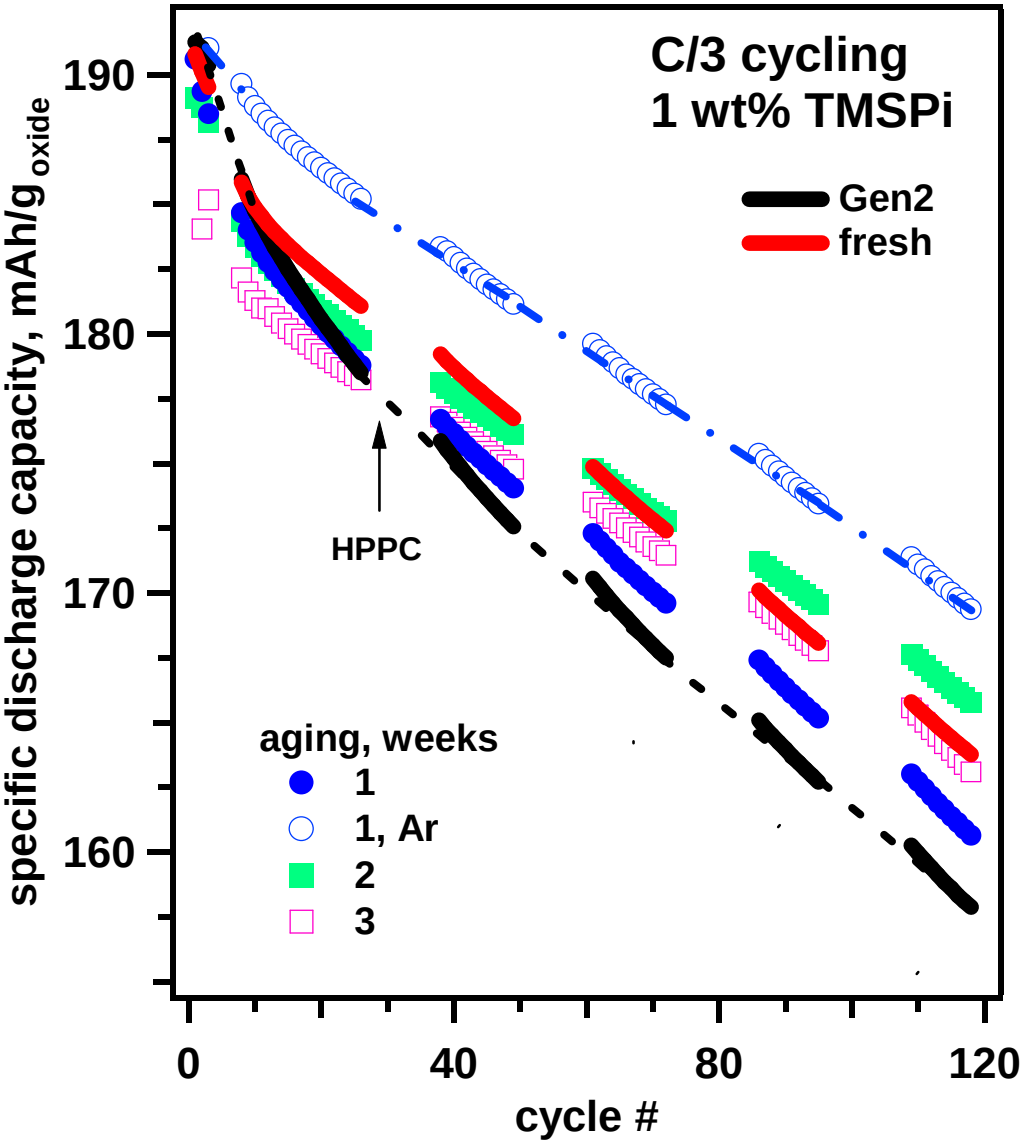

Figure S4. Capacity fade for C/3 cycling over 120 cycles for the baseline electrolyte (Gen2) and electrolyte solutions containing 1 wt% PX_3 and aged 0-3 weeks (symbols and solid lines, see the plot for disambiguation and color coding). Also shown is the trace for the Ar-bubbled solution aged over one week. The dash-dot lines are visual guides. The C/10, 1C, and HPPC measurements (see the arrow) interrupt the C/3 cycling (see Figure S1). C/10 data are shown in Figure 2.

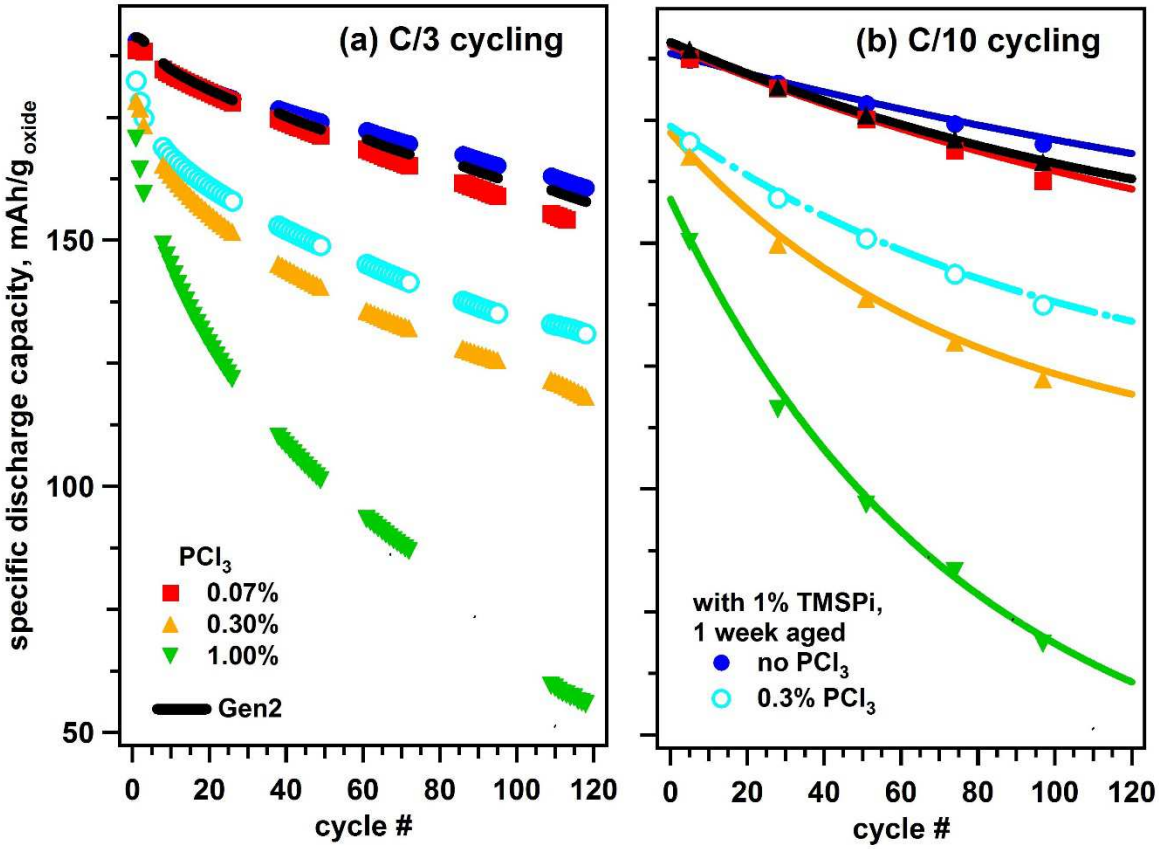

Figure S5. Rapid capacity fade observed in (a) C/3 and (b) C/10 cycling of the test cells (see the legend) containing PCl_3.

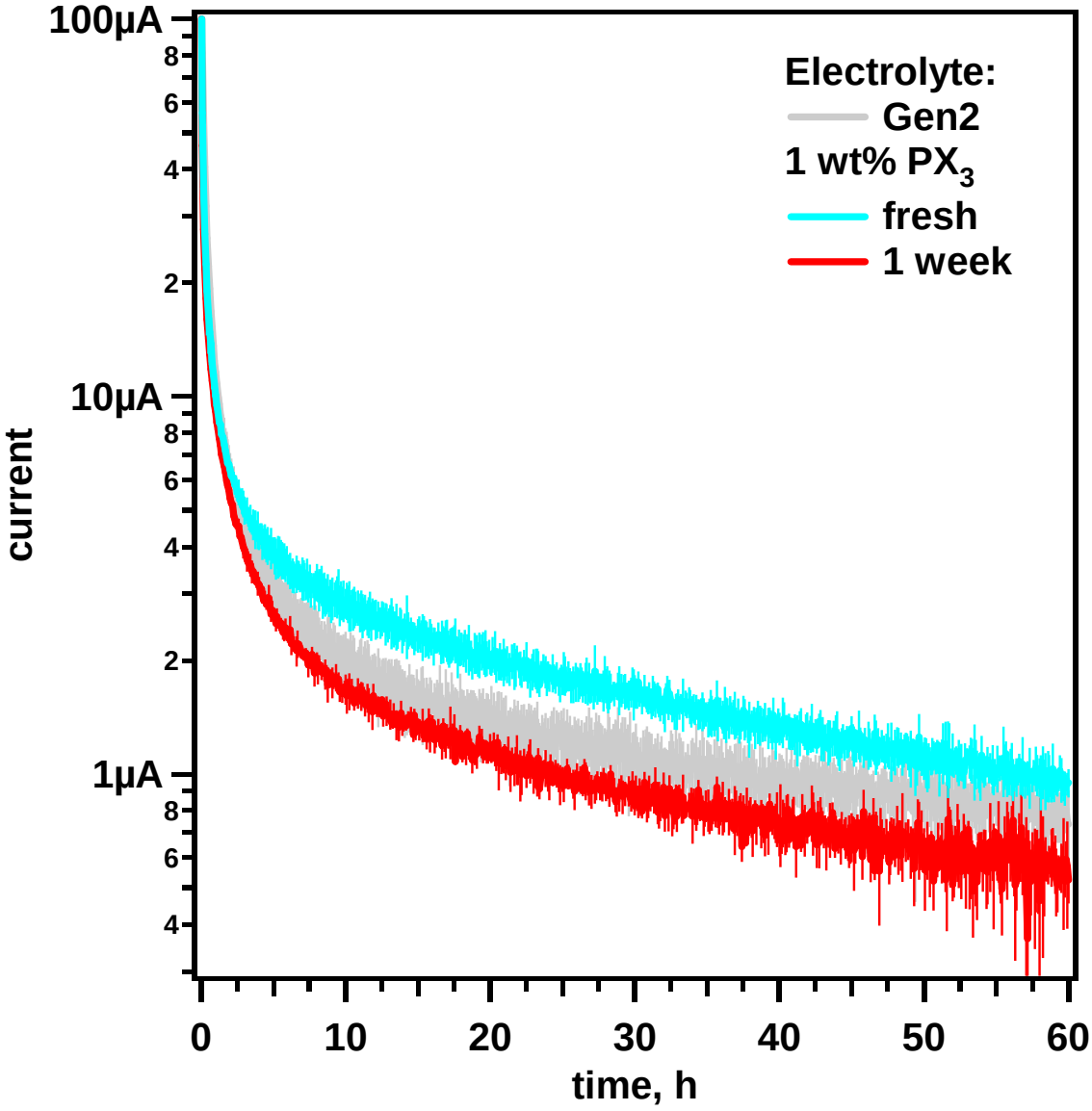

Figure S6. Current vs. time plot for the potentiostatic hold at 4.6 V vs Li/Li^+ for the cells containing Gen2 baseline electrolyte (*black line*) and the cells containing 1 wt% PX_3 before (*blue line*) and after one week of *ex situ* aging (*red line*). Each trace is the average of three identical coin cells, with the vertical bars indicating the standard deviation. Mind the logarithmic vertical scale.

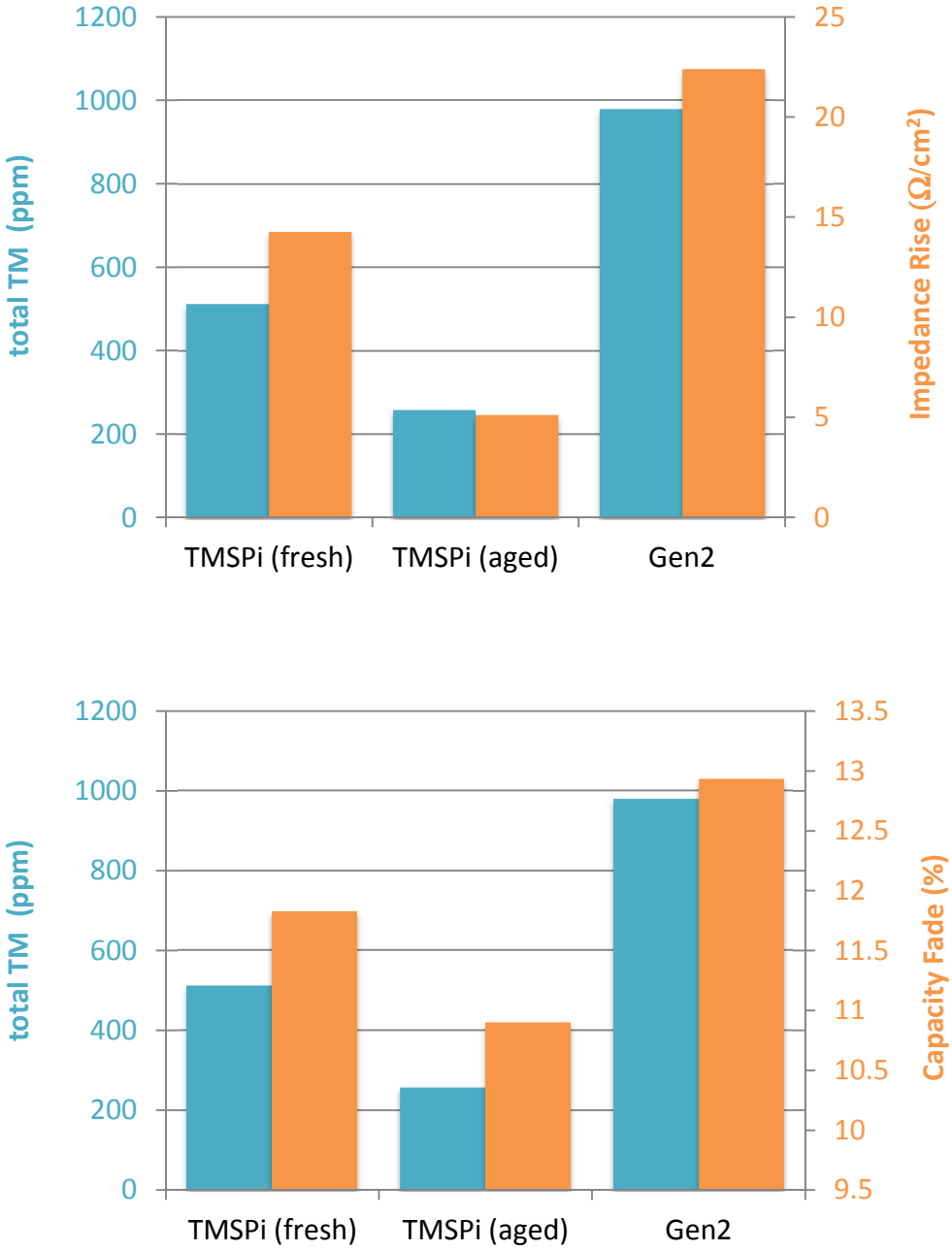

Figure S7. Correlations observed between the total concentration of transition metal (TM) ions deposited into the graphite electrode and the capacity fade (*top*) and the relative ASI increase at 3.7 V (*bottom*) after 100 cycles for the cells (i) containing Gen2 baseline electrolyte (*far right*) and (ii, iii) 1 wt% PX_3 in Gen2, before and after one week of *ex situ* aging.

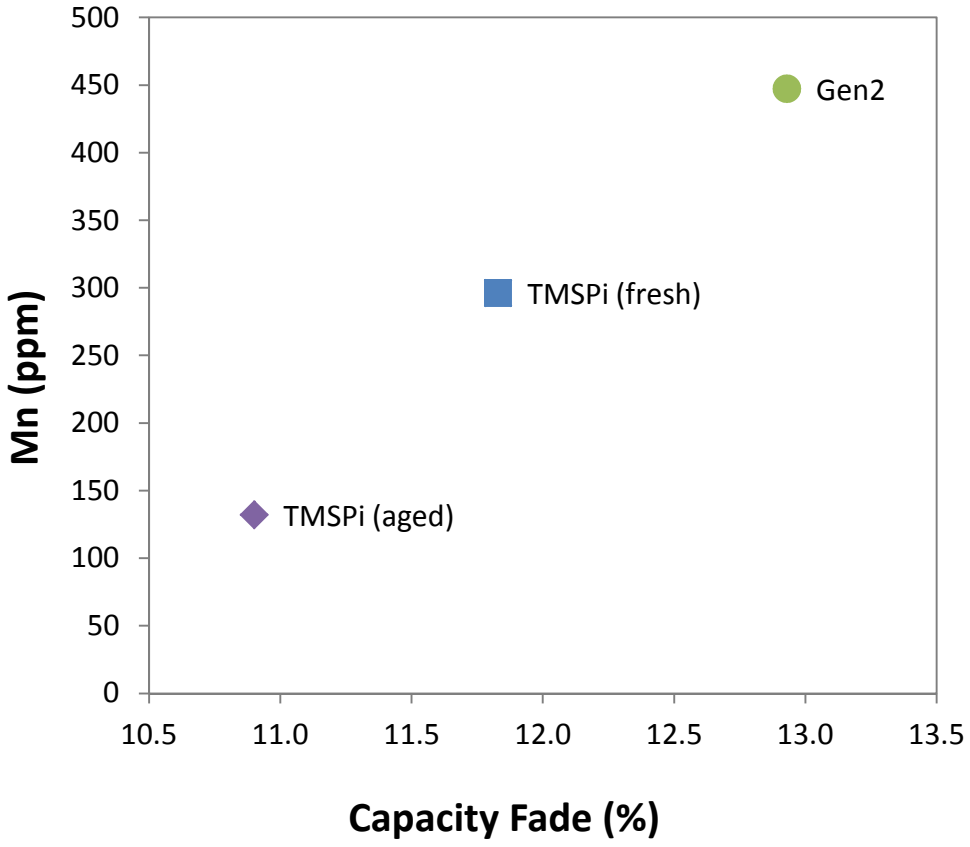

Figure S8. Correrlation betwee the concentration of deposited Mn in the graphite electrode with the capacity fade for the three cells shown in Figure S7.

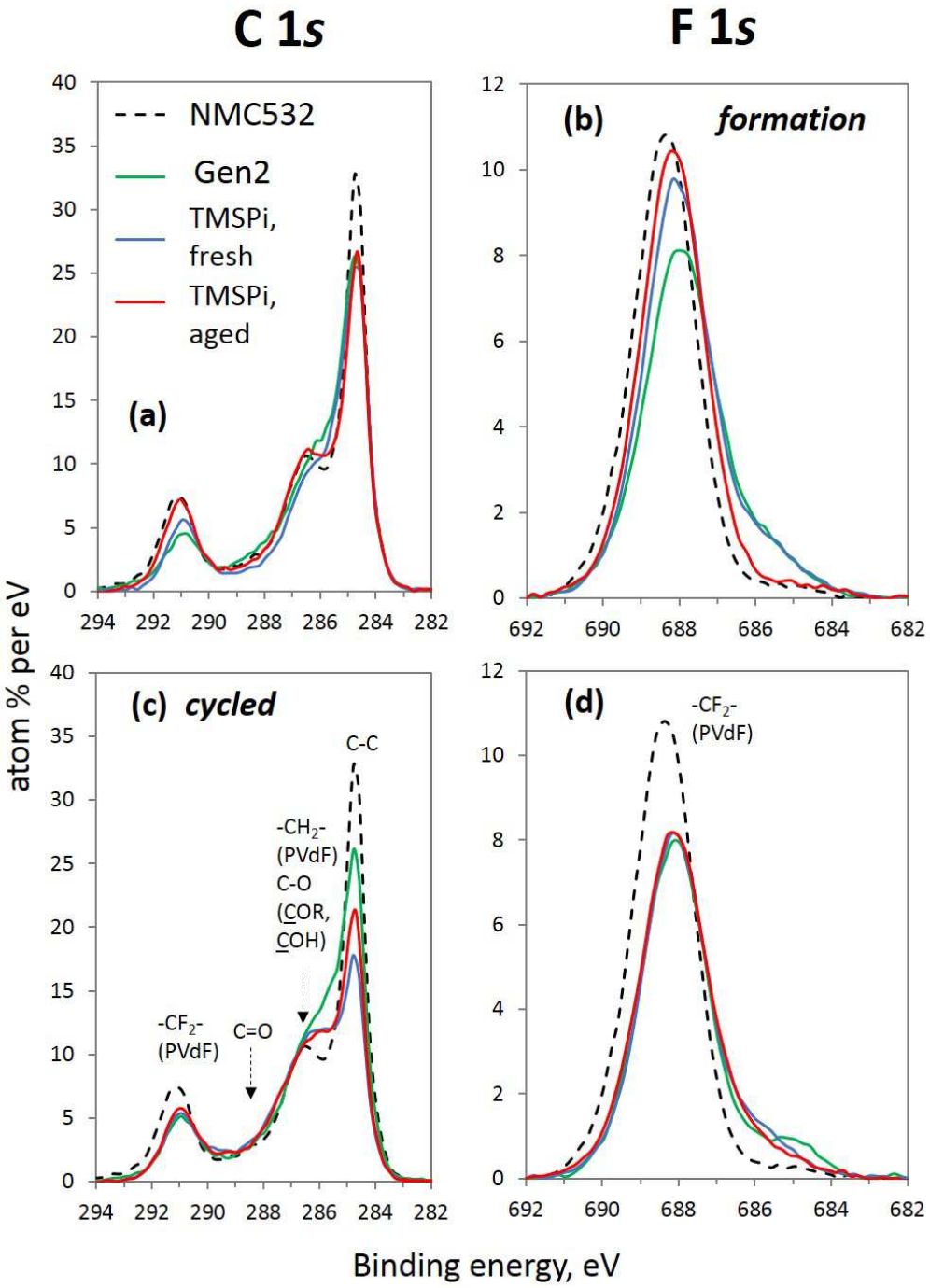

Figure S9. X-ray photoelectron spectra (XPS) in (a,c) C 1*s* and (b,d) F 1*s* photoemission bands for positive electrodes harvested from the cells after (a,b) four formation cycles and (c,d) 100 aging cycles. The spectra for the pristine NMC532 cathode and the cathodes harvested from Gen2 cells and PX_3 cells (1 wt%) are shown; the latter cells have been assembled either before or after one week of *ex situ* electrolyte aging. Selected emission bands are indicated in panels c and d.

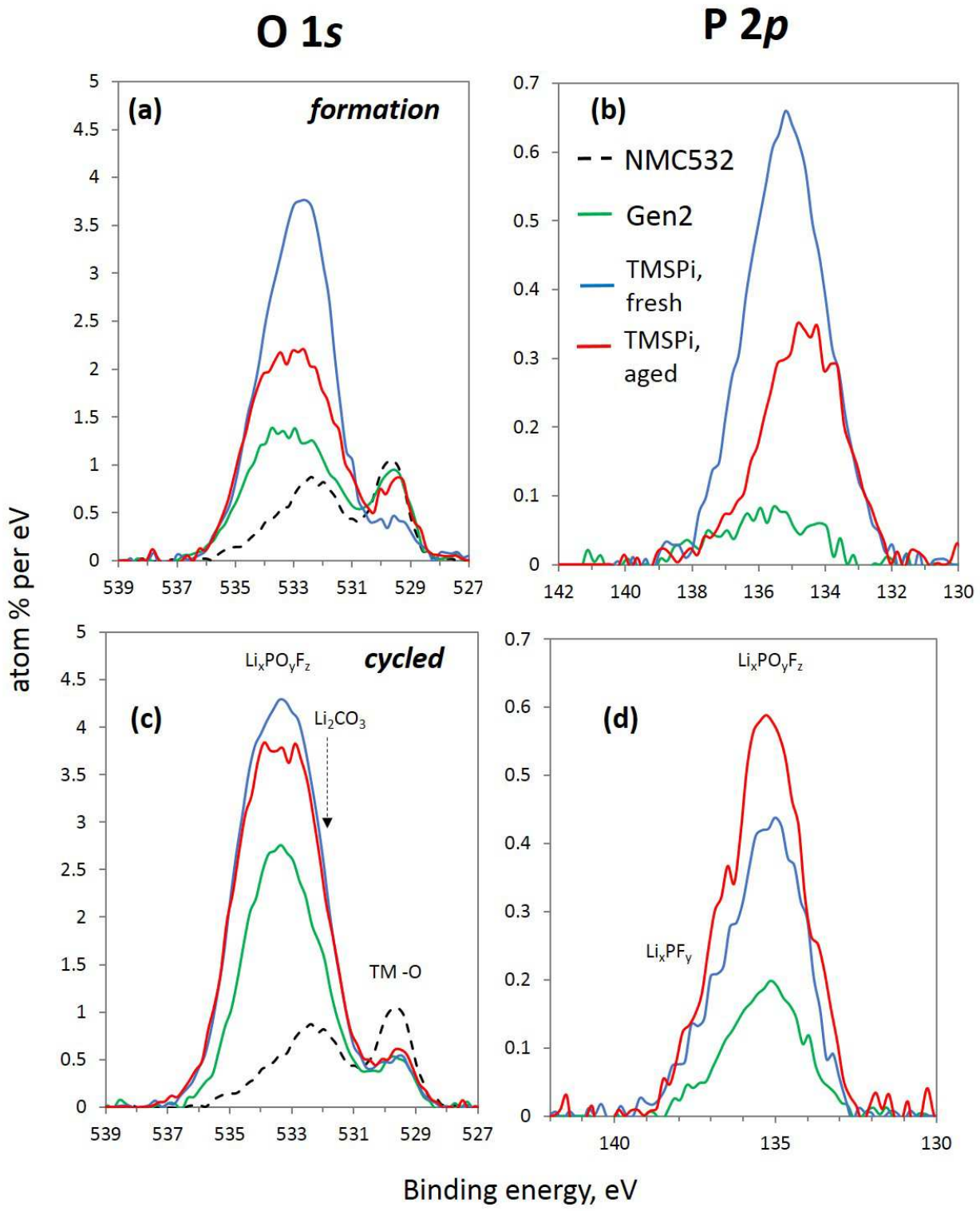

Figure S10. Like Figure S9, for (a,c) O 1*s* and (b,d) P 2*p* bands.

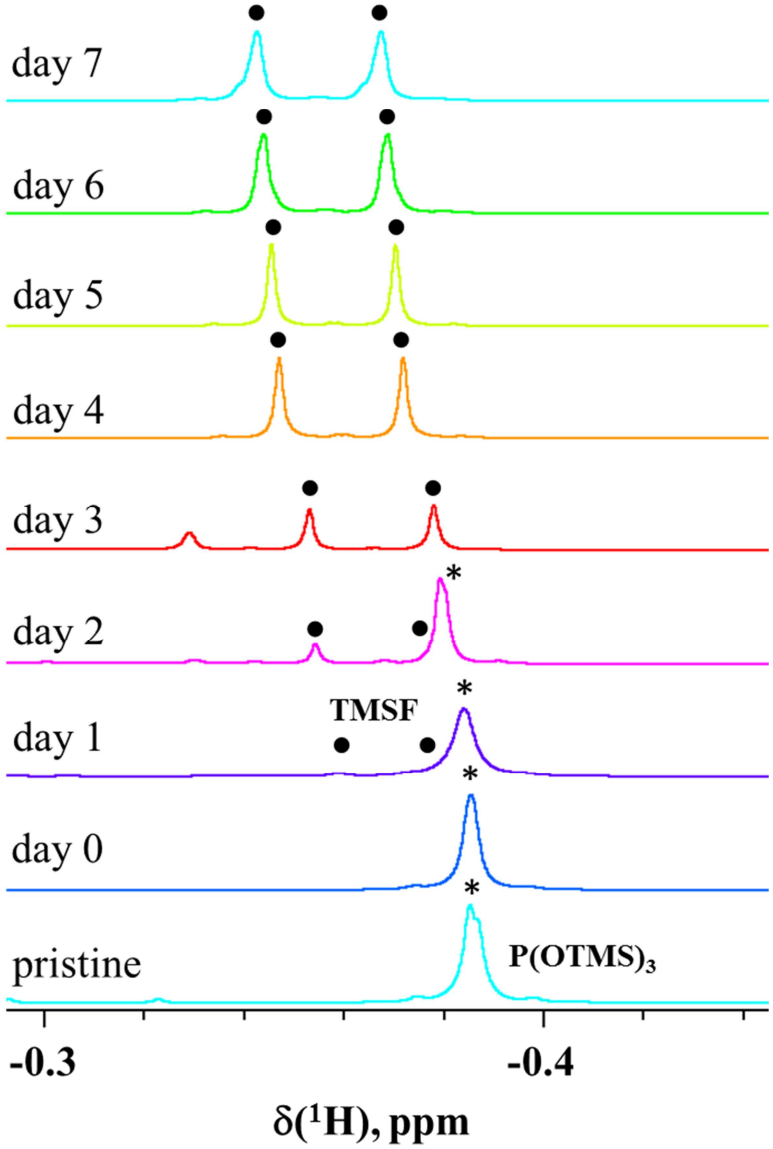

Figure S11. The progress of TMS elimination reaction observed by ^{1}H NMR spectroscopy (10 wt% PX_3 in Gen2). As the solution ages, the methyl resonance from PX_3 disappears and the ^{19}F-coupled doublets from TMSF (J_{HF} ≈7.4 Hz) gradually appear. By the seventh day, almost no parent compound is left in the mixture.

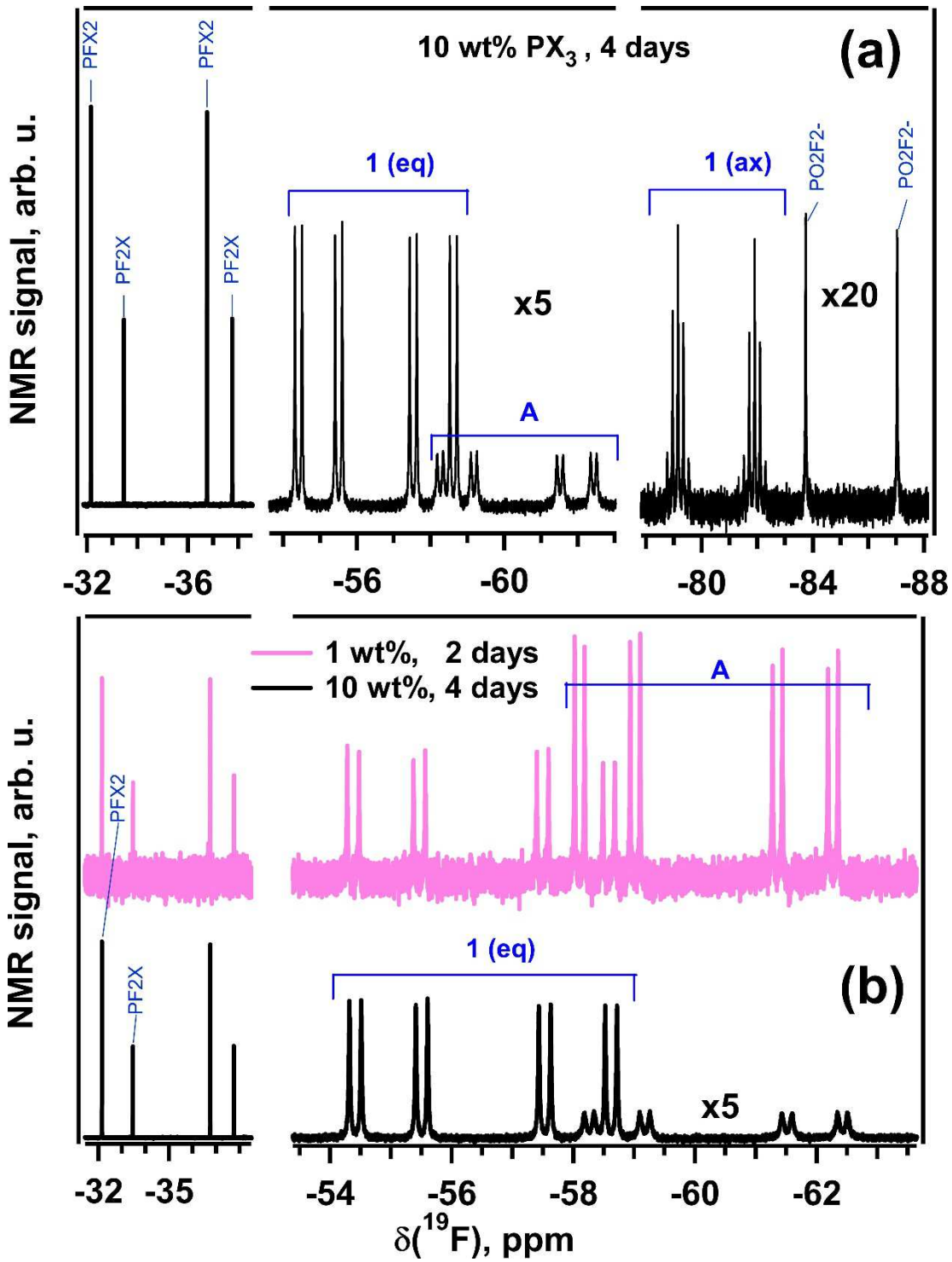

Figure S12. (a) Excerpts from the ^{19}F NMR spectrum of 10 wt% PX_3 in Gen2 after two day aging at room temperature. Note the magnification factors given in the plots. Multiplet A has *ddd* pattern (-60.35 ppm, *ddd*, *J*=914.8, 259.1, 48.2 Hz) that is similar to equatorial fluorines in **1** (-56.5 ppm, *ddd*, *J*=880.8, 307.6, 55.8 Hz). (b) At lower concentration of PX_3 and shorter aging periods, the progenitor of A occurs in preference to progenitor of **1**.

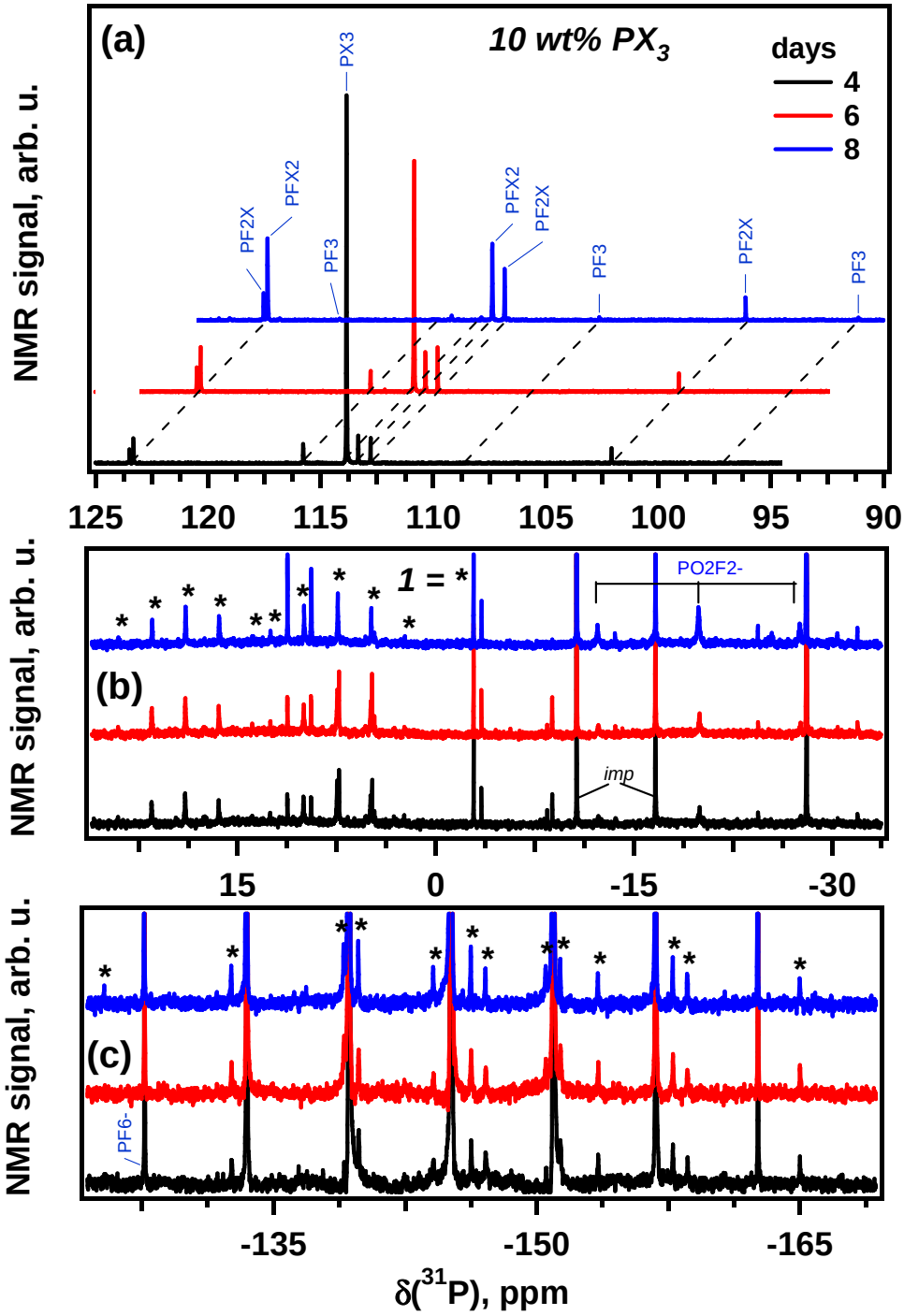

Figure S13. Evolution of ^{31}P NMR spectra for 10 wt% PX_3 solution aged for 4, 6, and 8 days (in different spectral regions). The asterisks indicate the resonance lines of **1** and "imp" indicates impurity in PX_3. Observe the decay of PX_3 in panel a (the traces have been shifted to facilitate comparison). PFX_2, PF_2X and (at 8 days) PF_3 are formed as the parent compound decays. In panel b, the triplet of $PO_2F_2^-$ is also indicated, and in panel c one of the seven equidistant resonance lines of PF_6^- is indicated (clipped).

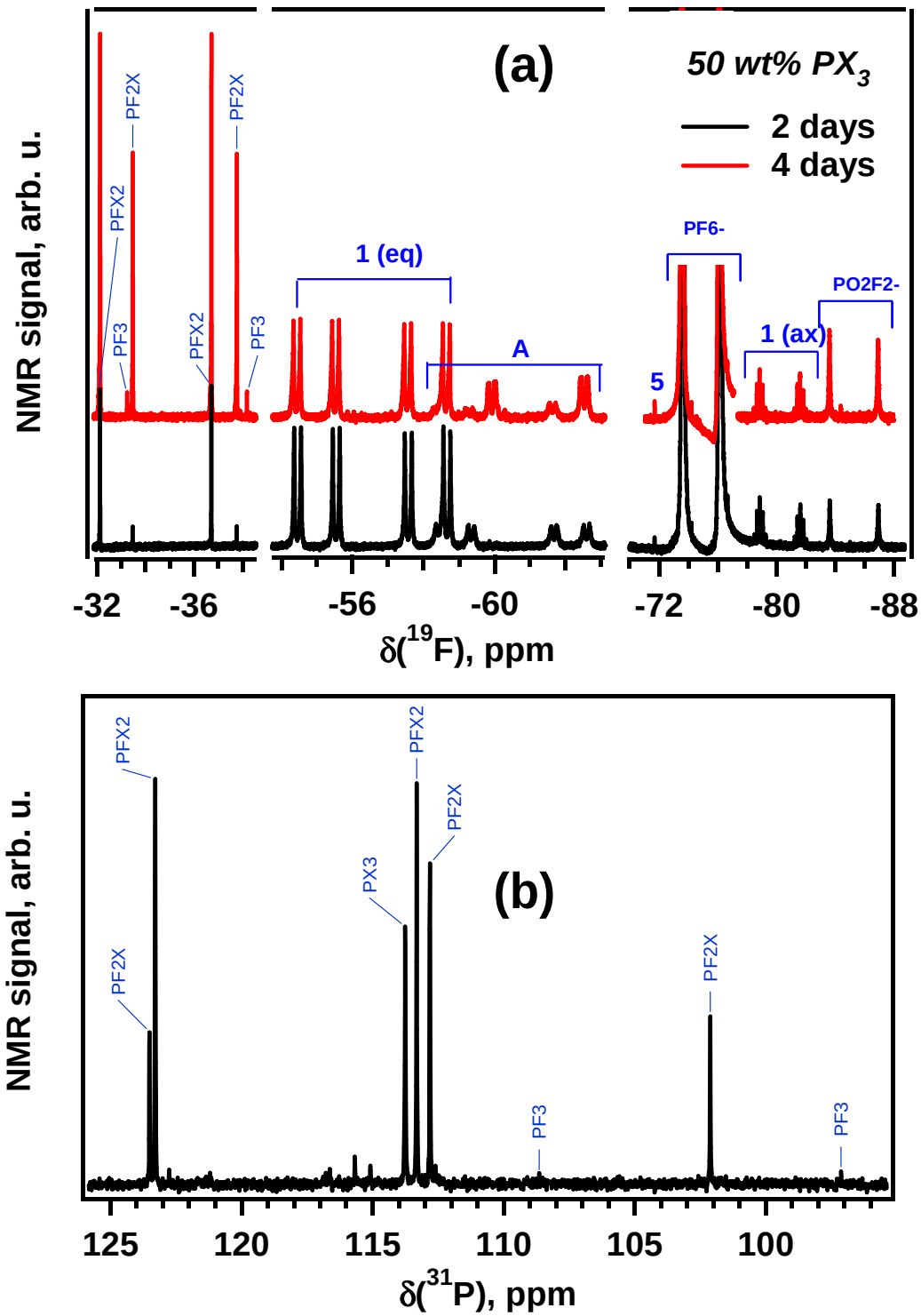

Figure S14. (a) ^{19}F and (b) ^{31}P NMR spectra of 50 wt% PX_3 solution in Gen2 aged for two (*black*) and four (*red*) days. Note that *ddd* multiplet A appears to split into two independent doublets.

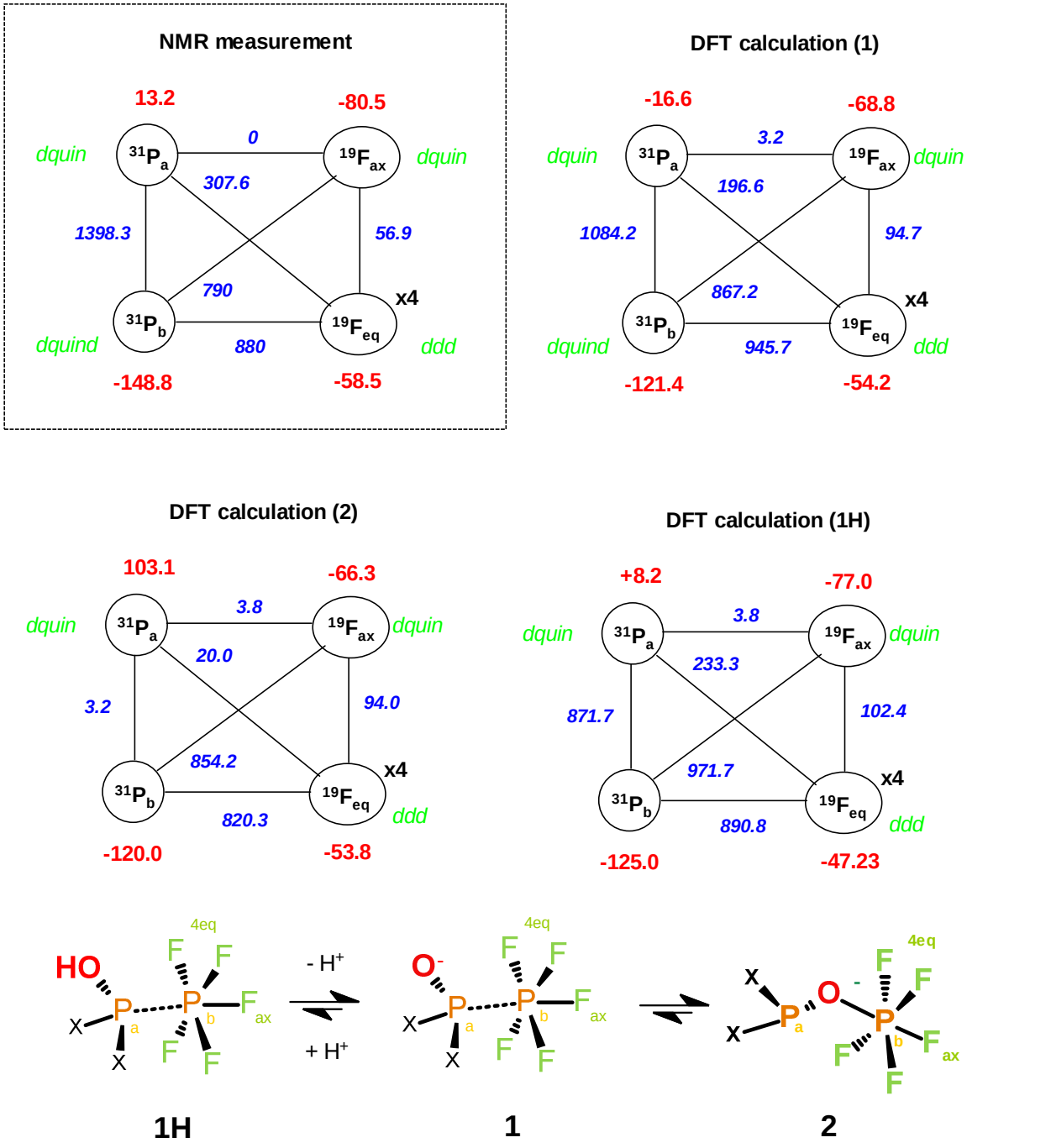

Figure S15. The ABCD system of compound **1** according to our NMR spectroscopy (*in the dashed rectangle*). Chemical shifts are given in red, multiplet patterns are given in green, and *J*-coupling constants are given in blue. Also shown are our DFT calculation for gas-phase anions **1**, its protonated form (**1**H) and μ-oxo bridged isomer **2**. Shown below is the postulated equilibrium between these three species (X=$OSiMe_3$).

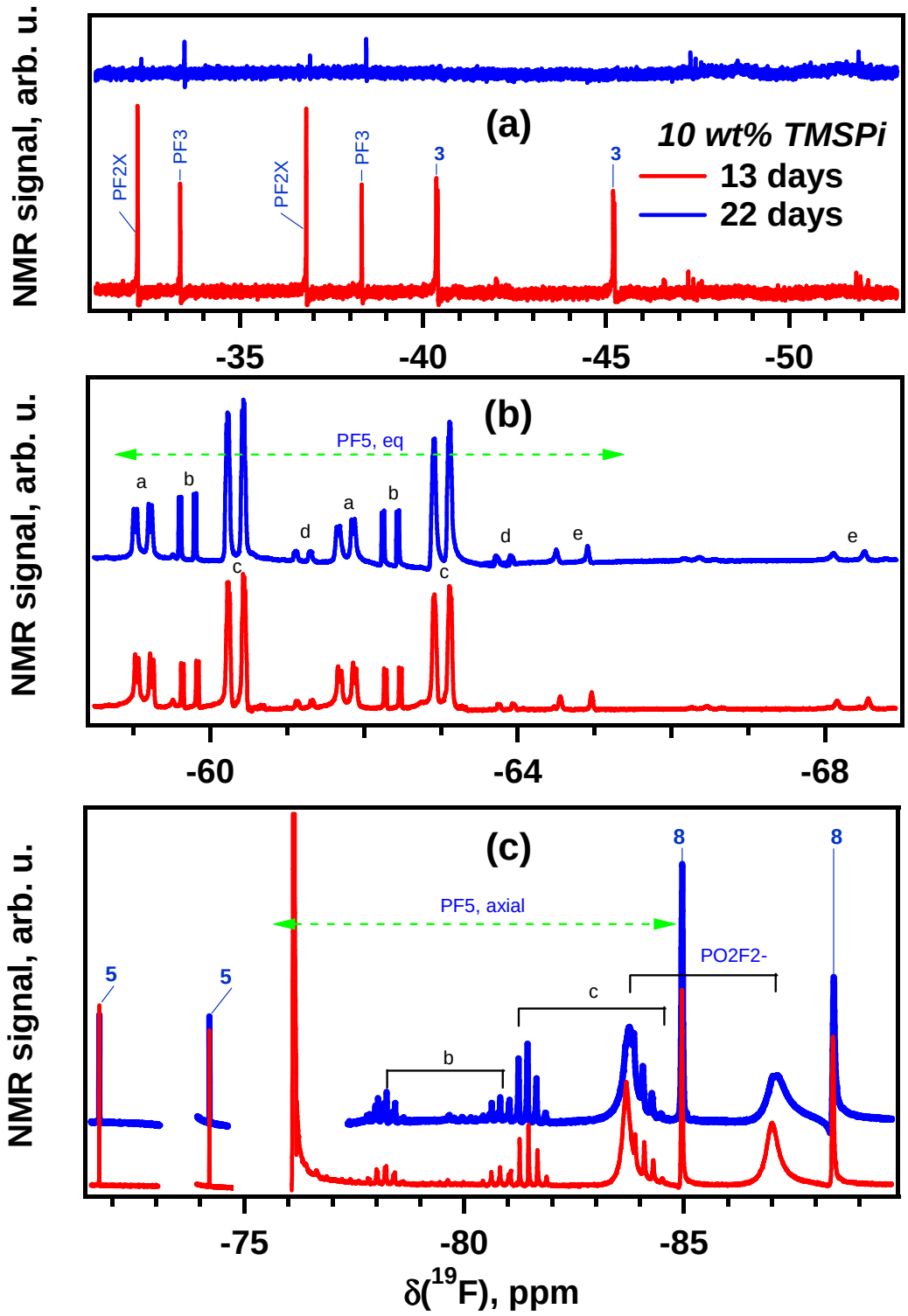

Figure S16. Excerpts from ^{19}F NMR spectra of 10 wt% PX_3 solution aged 13 and 22 days. P(III) species slowly decay as the solution ages (panel a), while most of P(V) species persist (panels b and c). Most of these P(V) species are PF_5Z^- species.

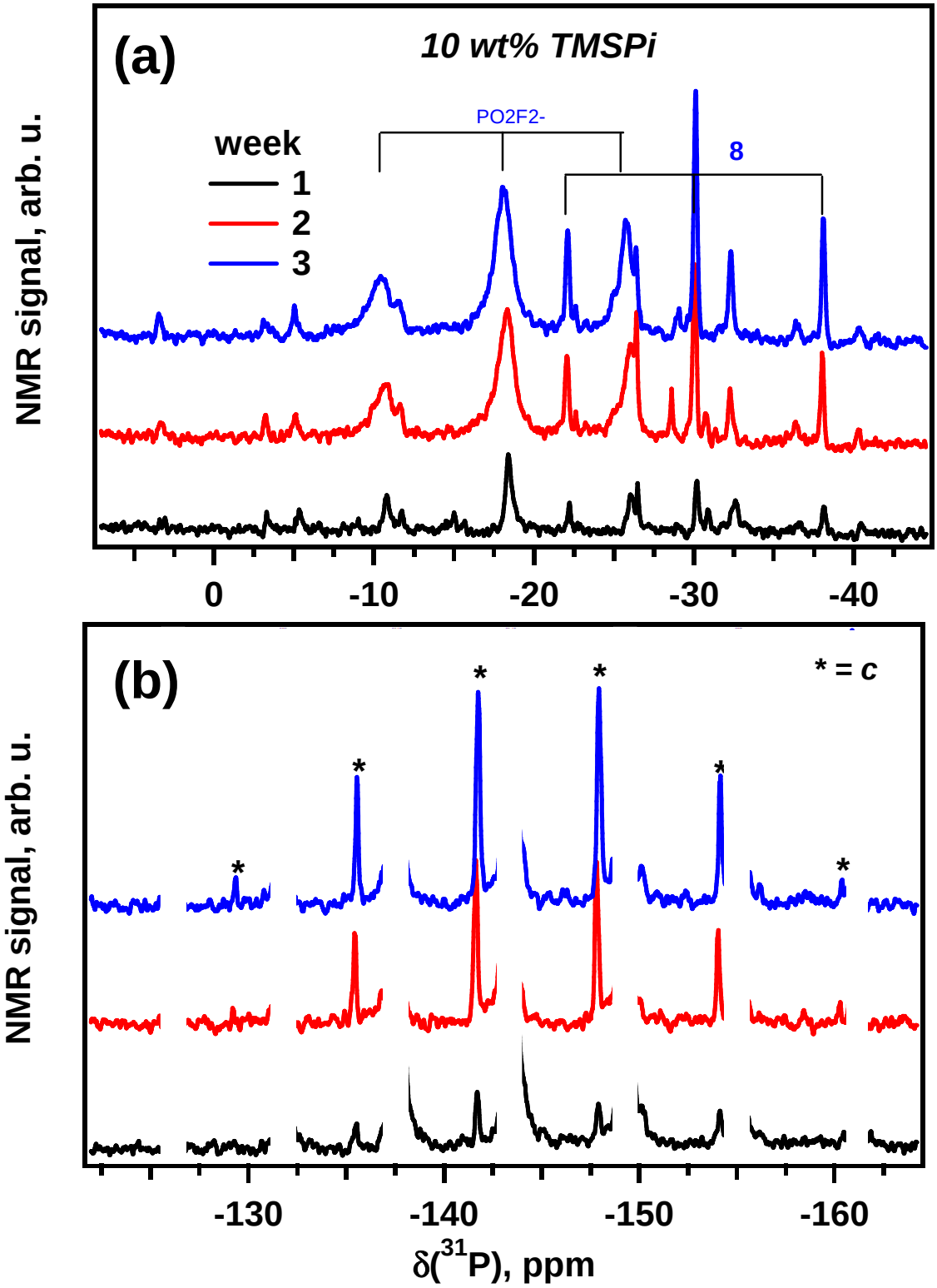

Figure S17. Excerpts from ^{31}P NMR spectra of aged 10 wt% PX_3 (1 to 3 week aging). The asterisks in panel b indicate phosphorus-31 resonances that correspond to progenitor of multiplets labeled c in Figure 7. The excluded resonance lines in panel b are from PF_6^-.

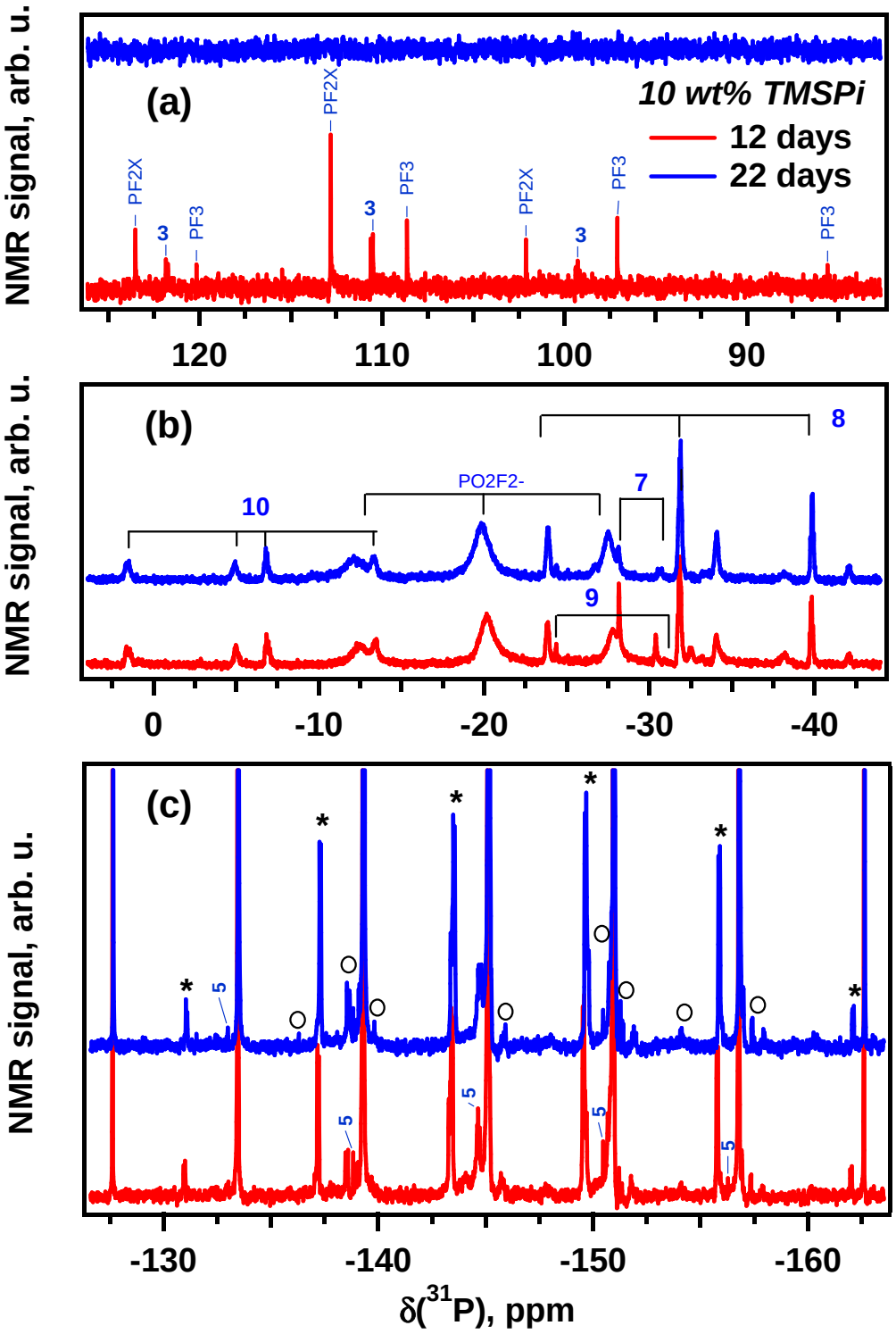

Figure S18. Like Figure S16 (another solvent aging experiment); ^{31}P resonances shown. In panel c, the asterisks indicate the most prominent PF_5-like species c (cf. Table S4). The doublet of **5** is also indicated, and the open circles indicate multiplet B (cf. Table S4).

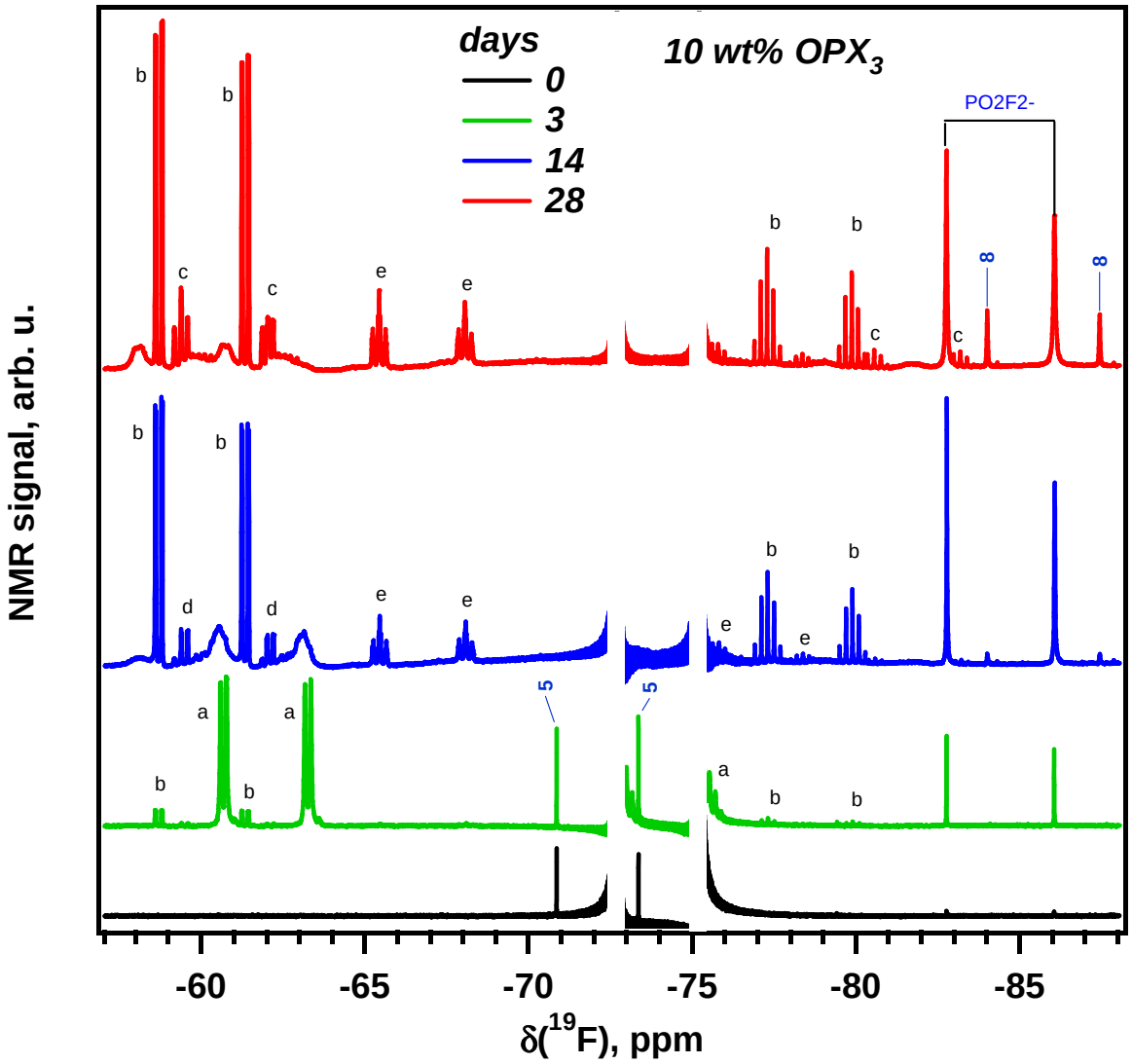

Figure S19. Time evolution of 19F NMR spectra from 10 wt% OPX_3 in Gen2 (0-48 days of aging). Only two spectral regions are shown, see Table S4 for other resonances. $PO_2F_2^-$, **5**, and **8** are observed in this solution, too, and there are also several PF_5-like species.

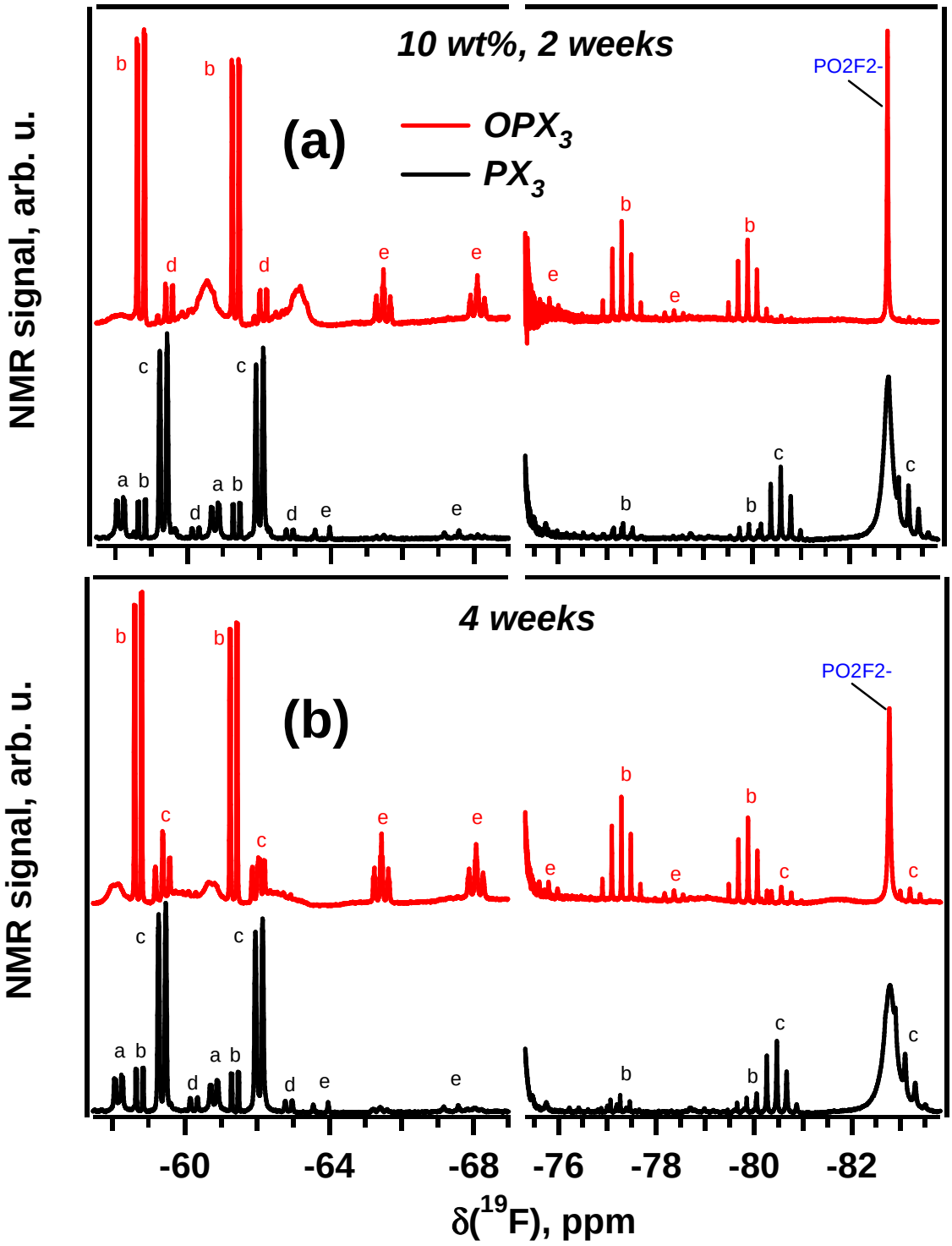

Figure S20. Comparison between ^{19}F NMR spectra of aged 10 wt% OPX_3 (red) and PX_3 (black) in Gen2 after (a) two and (b) four weeks. Multiplets b and c are almost identical in these two solutions.

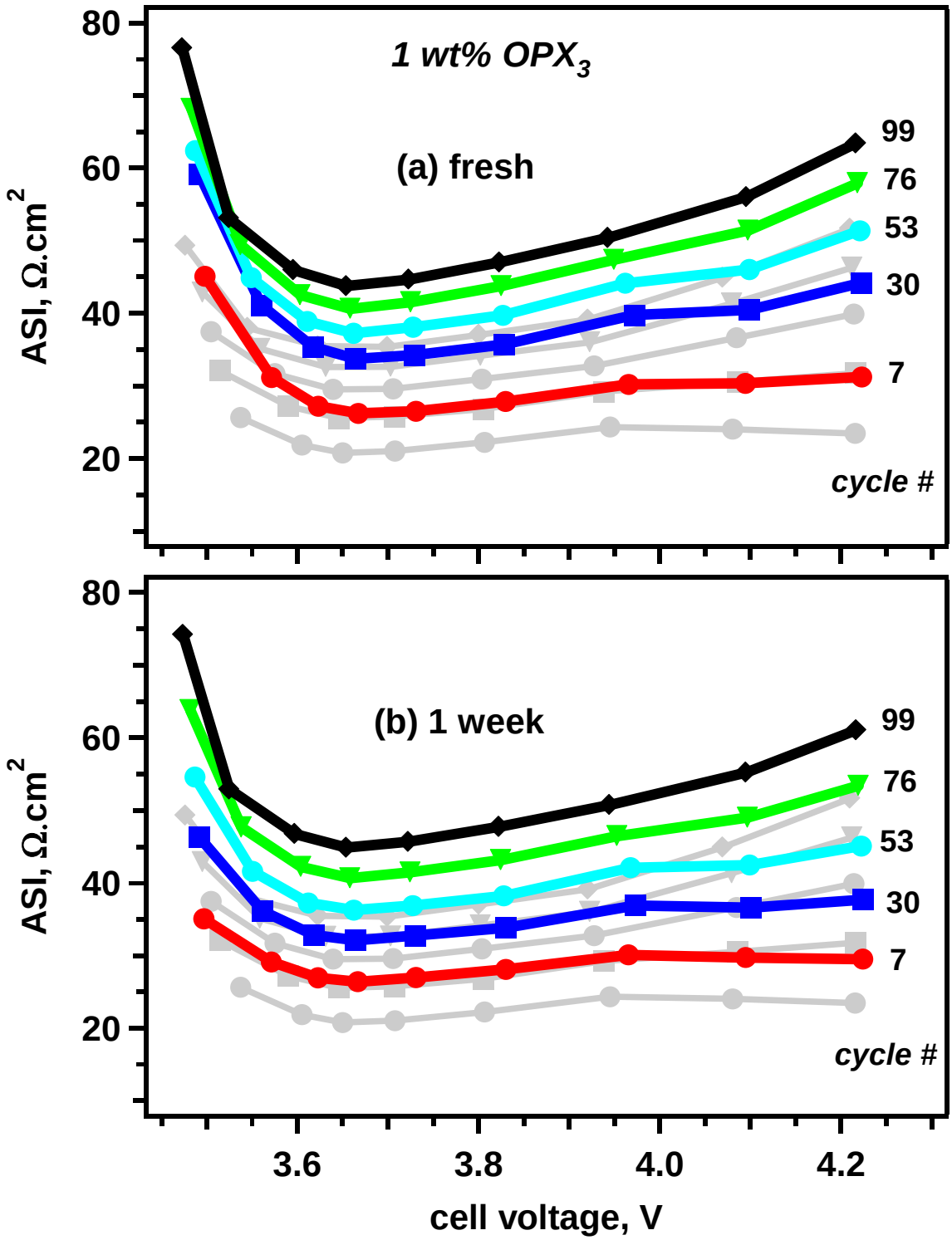

Figure S21. Like Figure 1 for OPX_3. No lowering in the impedance rise is observed in fresh or aged solutions of OPX_3.

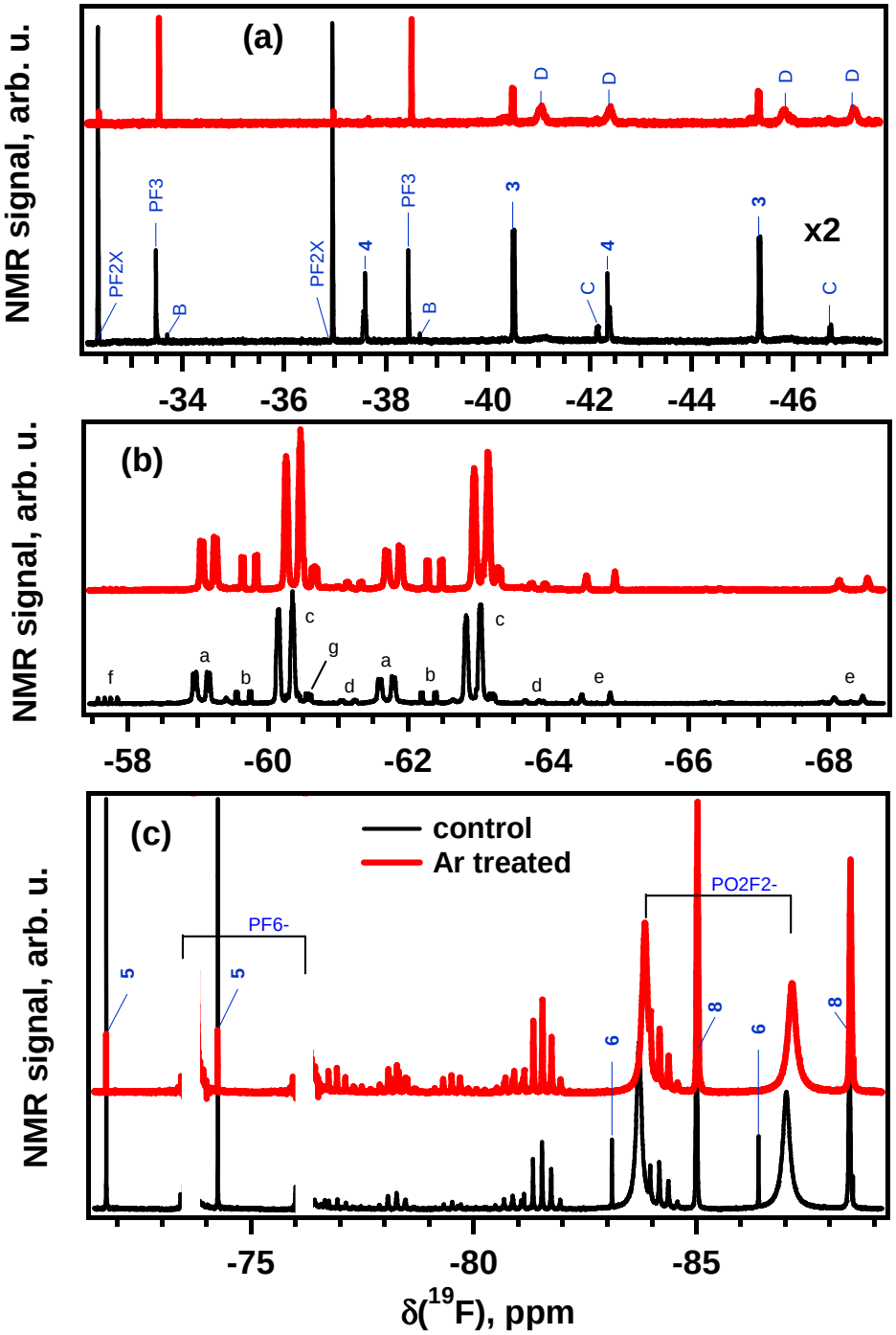

Figure S22. Comparison of ^{19}F NMR spectra from Ar bubbled and control 10 wt% PX_3 electrolyte solutions (one week aging; see Figure S23 for ^{31}P NMR spectra). Significant reduction in signals from PF_2X and PF_2-like species **3** and **4** is seen in panel a, and there is new multiplet D at -44.08 ppm (*dd*, *J*=1349, 378.7 Hz). All PF_5-like species are observed in panels b and c, the only missing feature is multiplet f. In panel c, product **5** is greatly reduced and **6** is missing entirely.

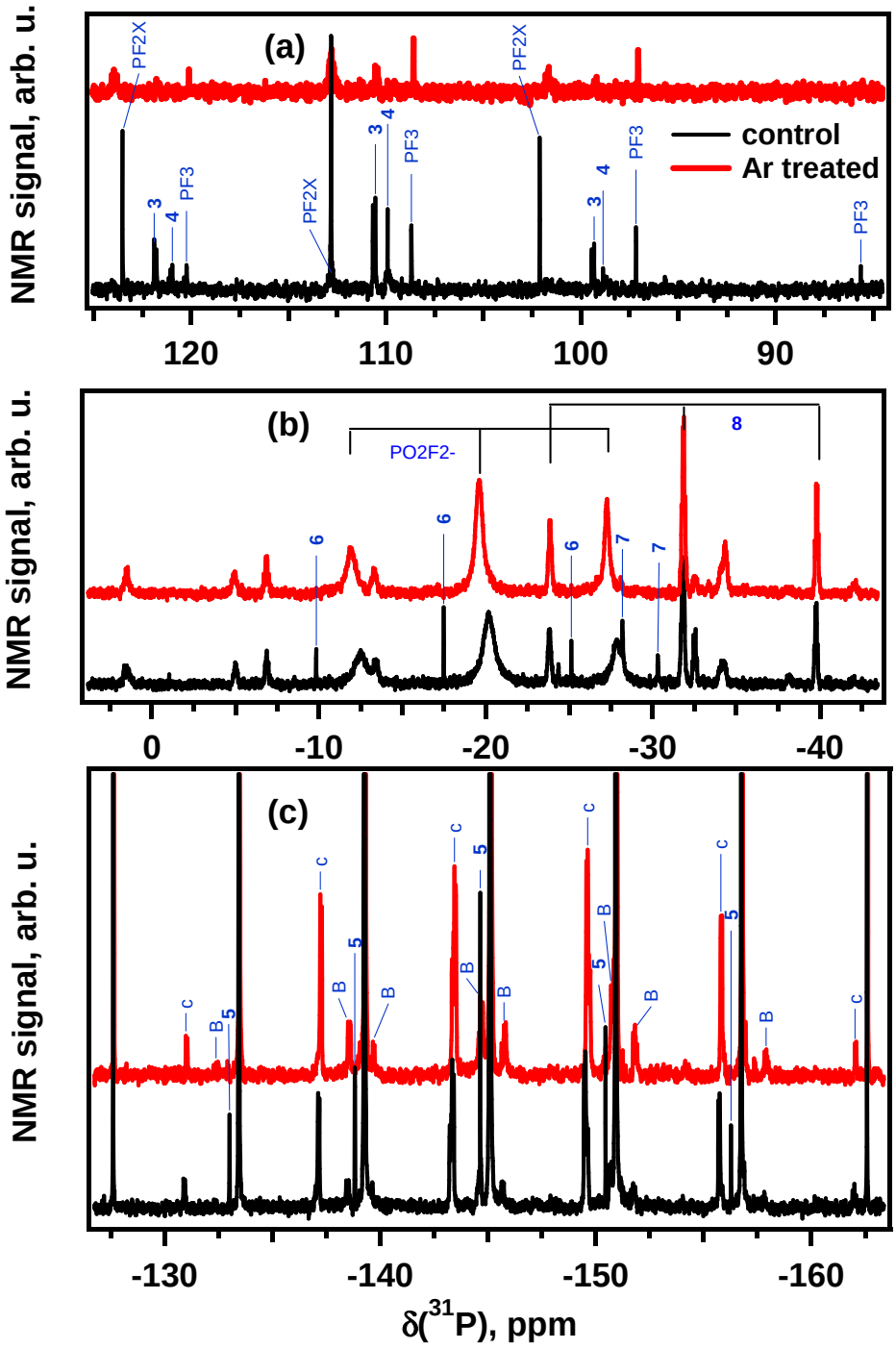

Figure S23. Comparison of ^{31}P NMR spectra from Ar bubbled and control 10 wt% PX_3 electrolyte solutions (1 week aging). Disappearance of triplets from PF_2X and **4** and reduction in **3** is seen in panel a, disappearance of **6** and **7** seen in panel b, and disappearance of product **5** in panel c. The signals were normalized to the multiplet from PF_6^-. Subsystems c and B correspond to *4dd* (-146.54 ppm, *J*=755.8, 742.7,9.5 Hz) an *dqd* (-145.28 ppm, *J*=877.4, 740, 15.5 Hz). The latter attribution is tentative, as the signal is weak.

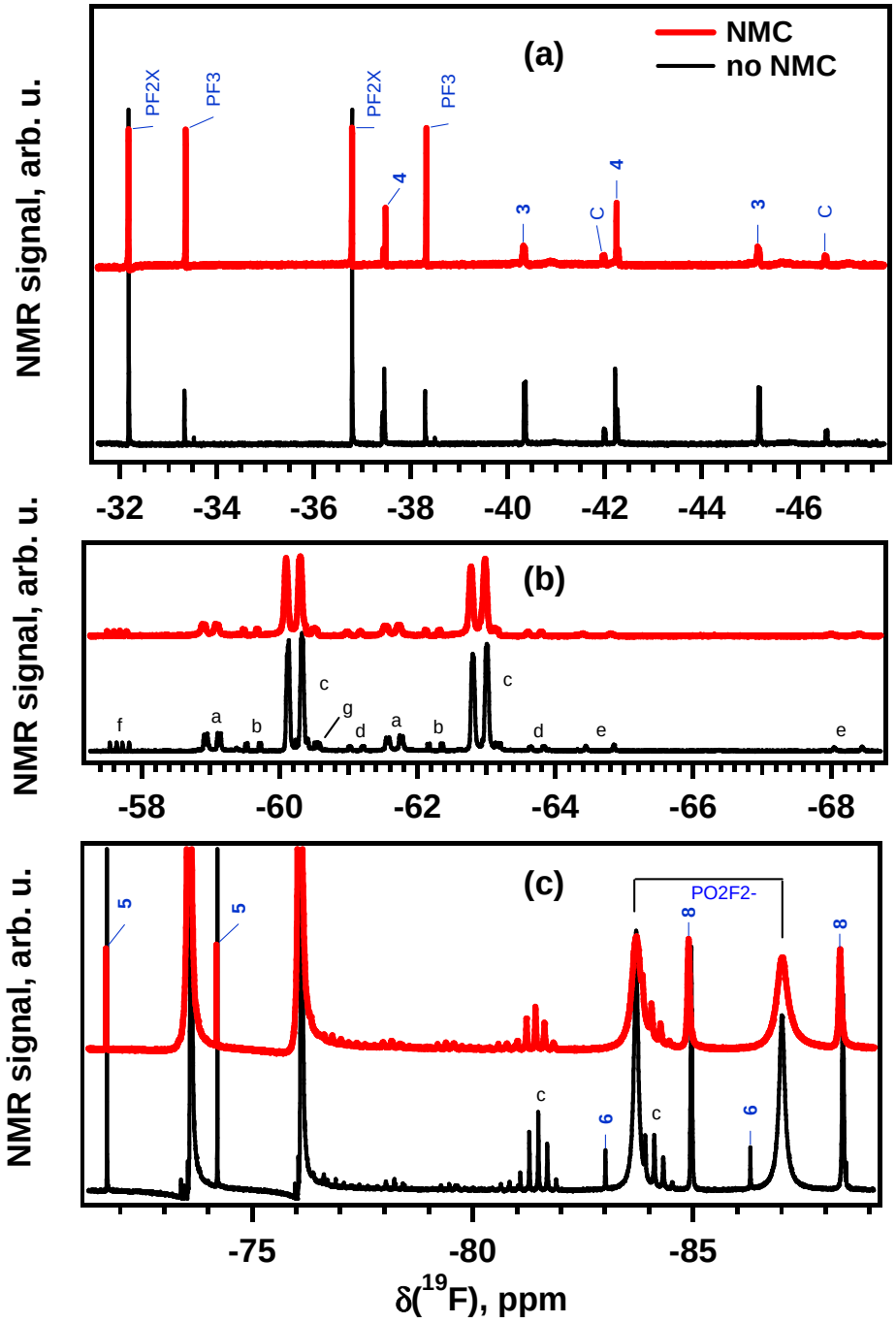

Figure S24. Comparison of ^{19}F NMR spectra from 1 week old 10 wt% $_{PX3}$ electrolyte solutions before and after exposure to NMC532 oxide (1 h stirring). Most of the resonances observed before the exposure are also observed after the exposure. The exceptions are products **5** and **6** that are also greatly reduced by Ar bubbling. None of the other P(V) species appear to be affected. Among the P(III) species in panel a, the exposure to NMC removes PF_2X and **3** in preference to PF_3 and **4**.

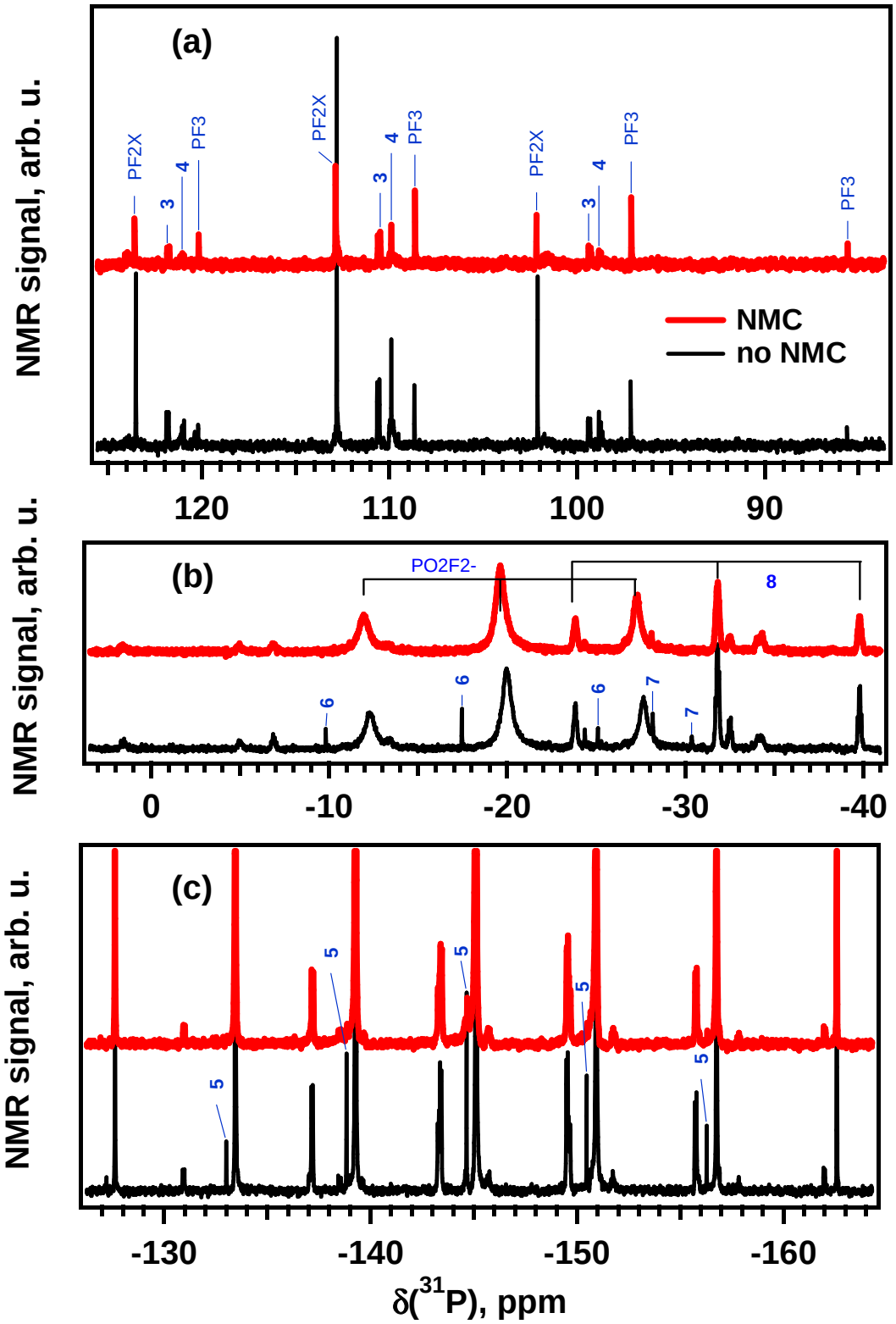

Figure S25. Like Figure S24; ^{31}P resonances. In panels c and b, resonance lines of products **5**, **6**, and **7** are indicated in the control traces.

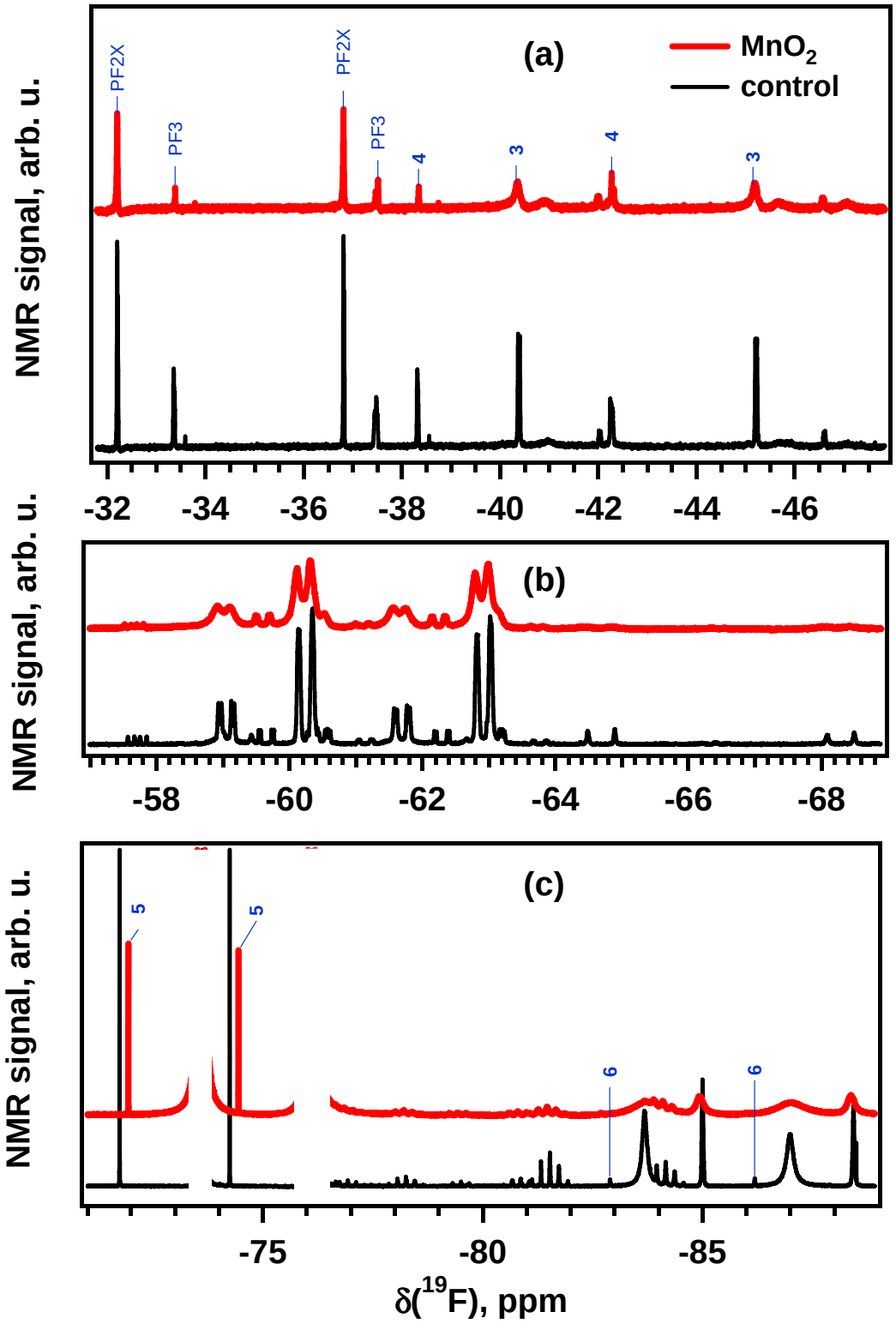

Figure S26. Like Figure S24, for MnO_2. The line broadening is due to the presence of Mn(II) ions in the solution.

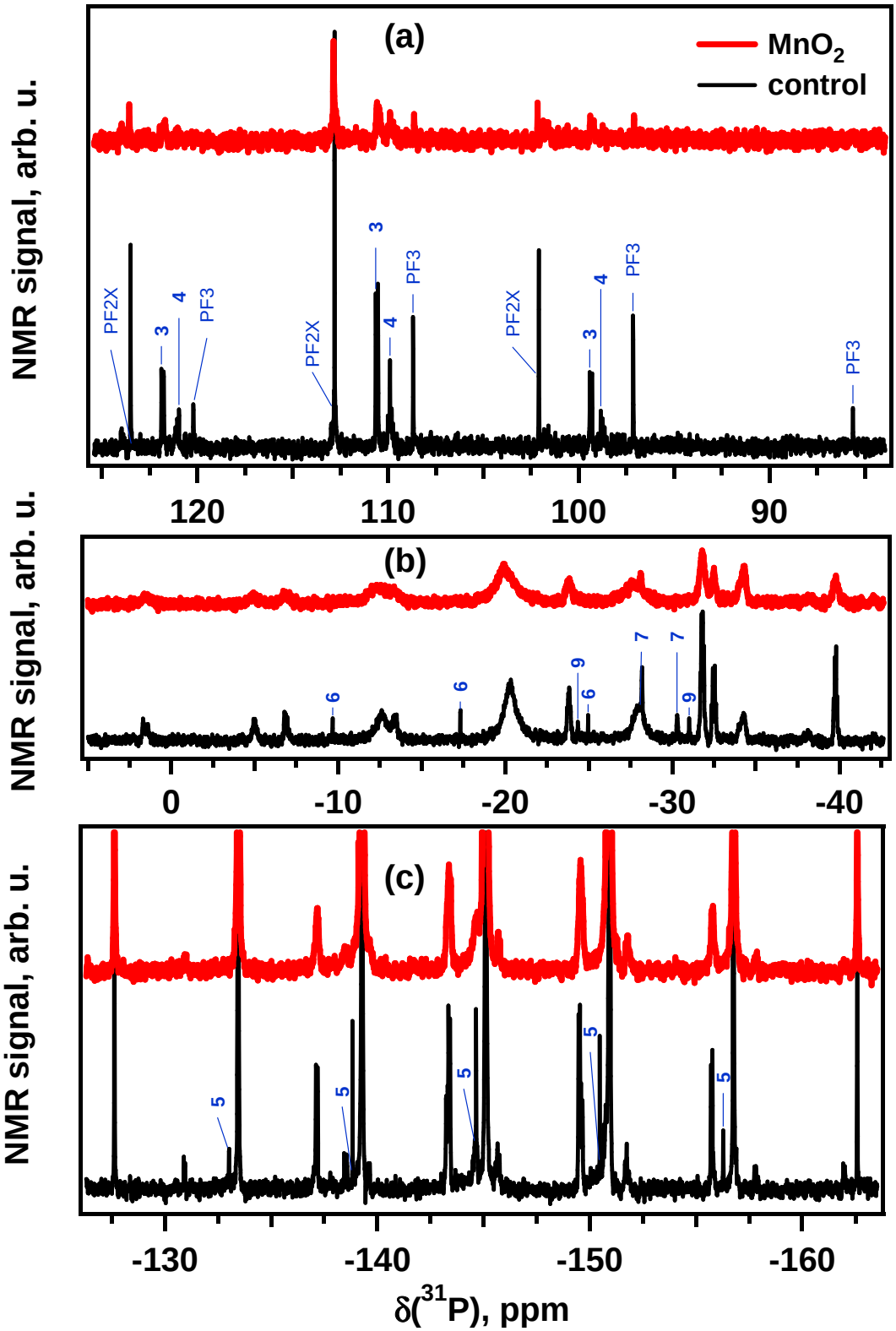

Figure S27. Like Figure S25, for MnO_2. The line broadening is due to the presence of Mn(II) ions in the solution.

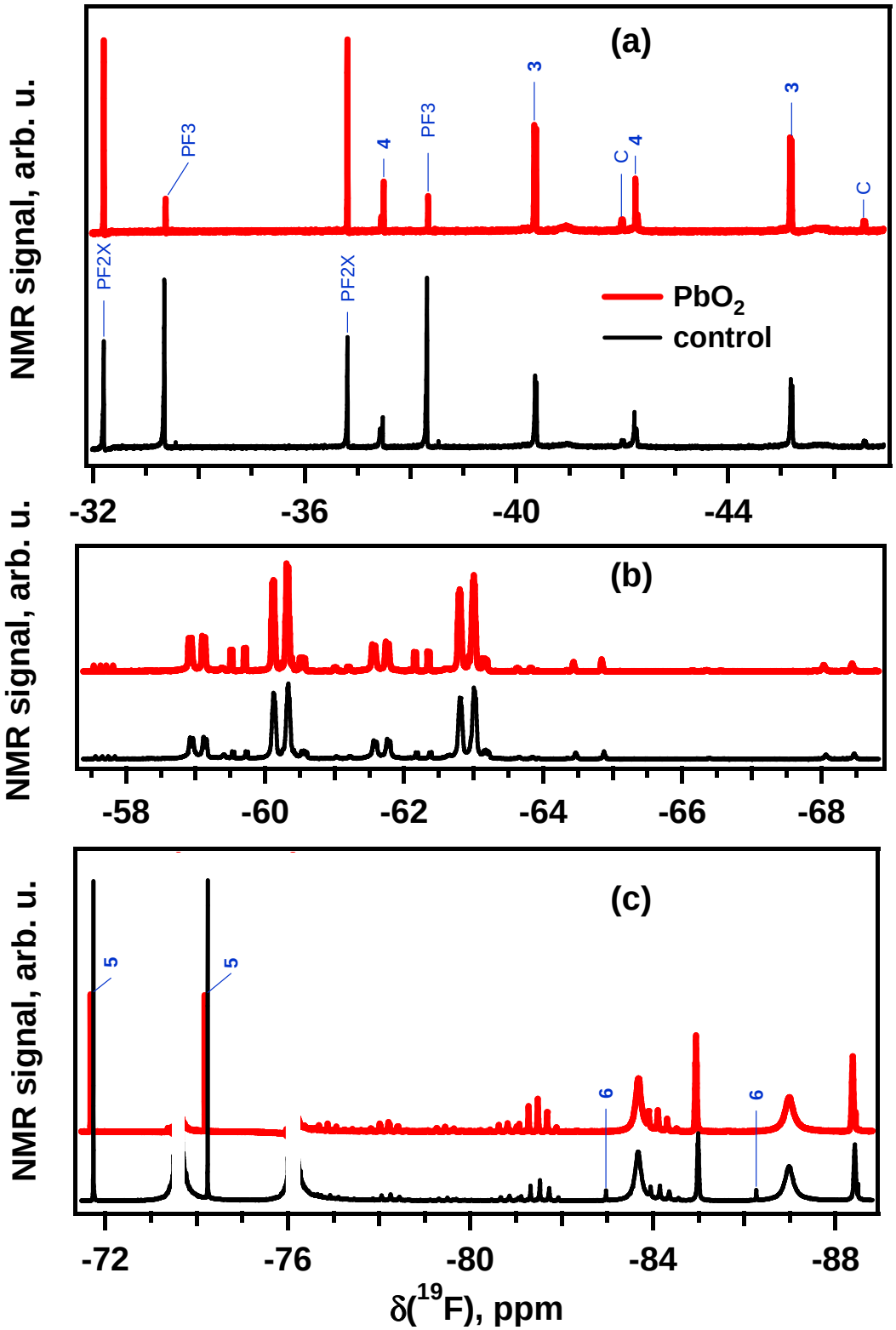

Figure S28. Like Figure S24, for PbO_2.

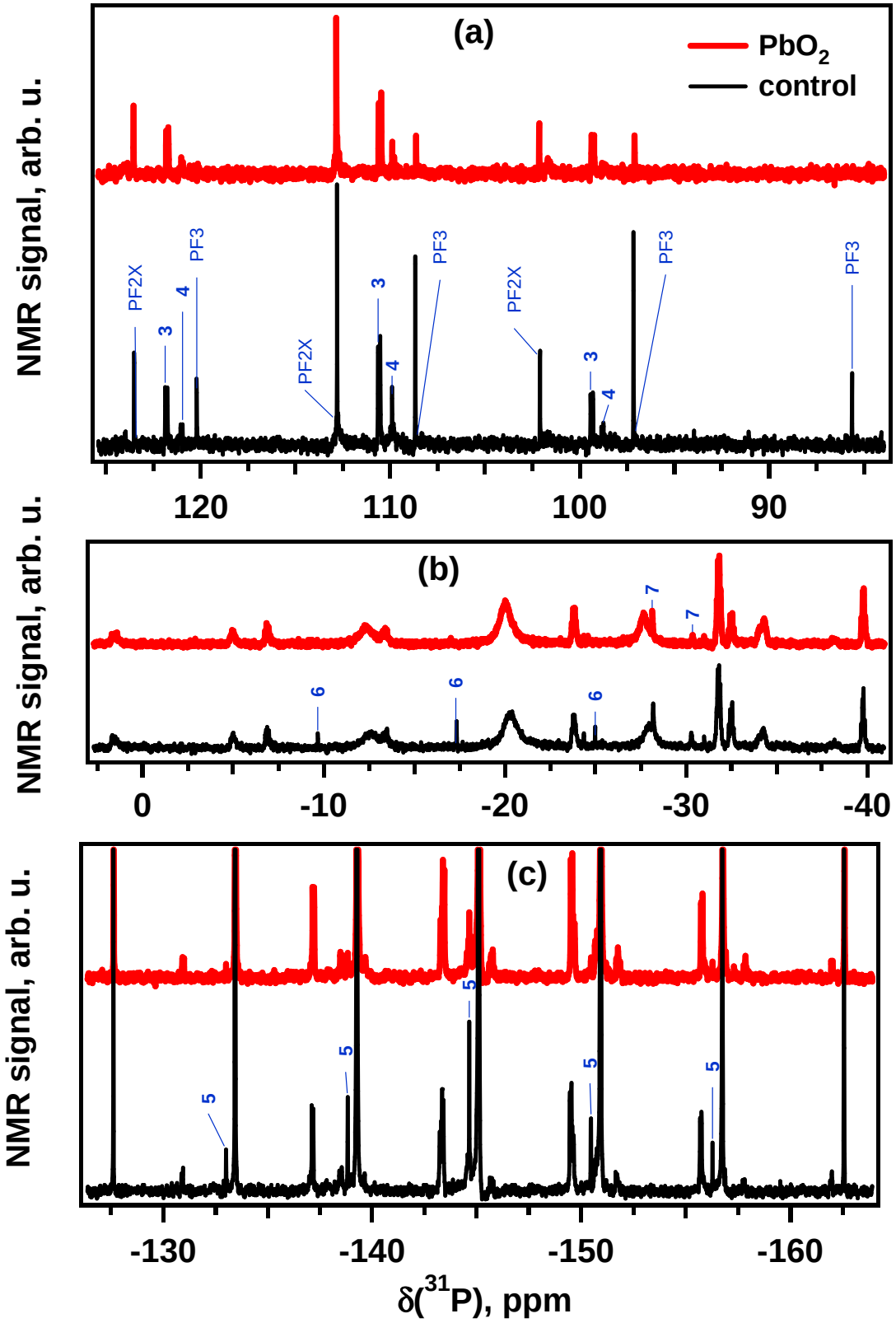

Figure S29. Like Figure S25 for PbO_2.

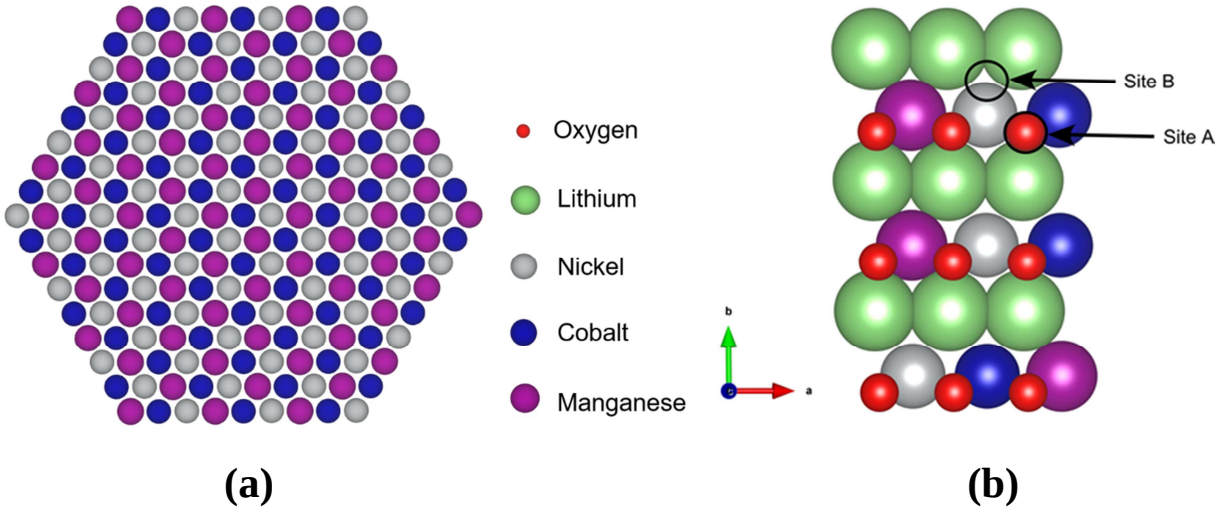

Figure S30. (a) Schematic representation of ion ordering in NMC111 layers and (b) top view of the (012) surface with 50% monolayer of oxygen coverage. The occupied sites are coordinated with two TM ions and one Li^+ ion (site A). The less favorable site B is indicated by an open circle.